Sensor and Simulation Notes

Note 427

November 1998

Design and Measurement of a Cassegrain-type Coaxial Beam-Rotating Antenna

Clifton C. Courtney, David Slemp, and William Motil
Voss Scientific
Albuquerque, NM

Carl E. Baum, Robert Torres, and William Prather
Air Force Research Laboratory / Directed Energy Directorate
Albuquerque, NM

Abstract

This paper describes the design and measurement of a Cassegrain-type, Coaxial Beam-Rotating Antenna (COBRA) designed and built to operate nominally at 3 GHz. The COBRA uses a set of reflecting surfaces to modify the usual pattern of radiation of an azimuthally symmetric aperture distribution (like the aperture distribution of a TM_{01} mode-driven conical horn) from a null along boresight (its axis) to one with a boresight peak. In addition, by slight alterations of the positions of the reflecting surfaces the boresight polarization radiated by the antenna described in this paper is adjustable, it can be linear or either sense of circular. The major components of the Cassegrain-type COBRA described in this paper include a TM_{01} circular waveguide mode driven conical horn, a parabolic main reflector, a hyperbolic subreflector, and a mechanical positioning system that allows rapid and automated adjustment of the antenna reflecting surfaces. In the first part of this paper a discussion of the design and fabrication of each of the major components of the Cassegrain COBRA is given, while the second part of the paper presents the results of extensive measurements taken to characterize the radiating properties of the antenna. The paper ends with a summary of the antenna's physical characteristics and a performance summary.

Table of Contents

1. INTRODUCTION **3**

2. SYSTEM CONCEPT **5**

2.1 FUNDAMENTAL PRINCIPALS 5

3. SEGMENT POSITIONING AND SYSTEM APPROXIMATIONS **7**

3.1 MODE CONVERSION 8

4. SYSTEM ELEMENTS **10**

4.1 MAIN REFLECTOR 10
4.2 SUBREFLECTOR 11
4.3 FEED HORN 12
4.4 PETAL POSITIONING SYSTEM 13
4.4.1 Asymmetric Scissors Jack *14*
4.4.2 Linear Actuator *16*
4.4.3 Actuator Controller *16*
4.4.4 System Computer *17*
4.5 SURFACE PROFILE MEASUREMENT AND VERIFICATION APPARATUS 17

5. MEASURED PERFORMANCE DATA **21**

5.1 FEED HORN AND COBRA II INPUT IMPEDANCE 21
5.2 FEED HORN PATTERN AND RADIATION CHARACTERISTICS 23
5.3 N = 1 PATTERNS 24
5.4 N = 2 PATTERNS 26
5.4.1 Horizontally Polarized Boresight Field *28*
5.4.2 Vertically Polarized Boresight Field *31*
5.5 N = 4 PATTERNS 33
5.6 N = 4 BORESIGHT PHASE RELATIONSHIPS 39

6. COBRA SYSTEM SUMMARY AND CONCLUSIONS **41**

7. REFERENCES **43**

Acknowledgement - This work was sponsored by the United States Air Force under a Small Business Innovation for Research Phase II program, contract no. F29601-97-C-0005.

1. Introduction

This paper describes the design and measurement of a prototype 3 GHz, Cassegrain-type, Coaxial Beam-Rotating Antenna (COBRA), the COBRA II. The motivation for the antenna's design is twofold. First, the antenna will produce a boresight peak from an azimuthally symmetric aperture polarization. Second, the boresight polarization of the antenna is adjustable and will produce linear or circular polarization on boresight. Regarding the first, it is well known that many high power microwave (HPM) sources produce energy that leave the generation region in azimuthally symmetric transmission line modes [Ref 1, 2]. Antennas like the COBRA II can be attached in-line with a transmission line supporting azimuthally symmetric modes (TEM coaxial cable) or waveguide (TM_{01}-mode circular waveguide) to produce a pattern peak that is on the axis of the source and antenna. This is not the case with existing antennas that produce peaks off the physical axis of the source, and pattern peak locations that are functions of frequency [Ref. 3, 4]. Additionally, since the COBRA's topology tends to spread the energy density over a large area (relative to other antenna designs), the peak electric field in the volume of the antenna and vacuum/air interface region of the system should be reduced to levels that will reduce the likelihood of electrical breakdown and possible pulse shortening of the HPM source [Ref. 5, 6]. Regarding the second, if the system designer's goal is to project microwave energy across a distance and couple it into systems with unknown or changing (rotating) aperture orientations, then circular polarization (or polarization agility) offers the greatest probability of success since the radiated field rotates with time (for circular polarization). When compatibility with an HPM source and the need to optimize coupling are the paramount considerations, the Cassegrain COBRA design is the superior antenna choice. The remainder of this section provides an overview of the contents of each section of this note.

The COBRA II, shown in Figure 1, uses a parabolic main reflector that is partitioned into four equal segments, and a hyperbolic subreflector that is illuminated by a conical horn driven by the TM_{01} circular waveguide mode. The next section of this note presents a brief overview of the fundamental concepts of the COBRA II design. The antenna is supplied with microwave energy by a circular waveguide propagating the TM_{01} mode. Without modification, the resulting aperture distribution would produce a null on boresight. But the COBRA II described here is capable of transforming the azimuthally symmetric aperture distribution of the circular waveguide into a distribution that will produce a boresight peak with a user-selectable polarization characteristic. To accomplish these properties, each segment of the main reflector is axially translated and rotated in a prescribed manner so that RF energy propagated through the system along different paths experience a different path length as it travels from the feed horn, to the subreflector, to each quadrant of the main reflector, and on to the antenna aperture plane. For the case where all four segments of the main reflector are positioned to form a standard parabolic surface, the antenna radiates a boresight null. For the case where two (adjacent) of the four segments of the main reflector are translated and rotated equally, linear polarization on boresight results, with either horizontal or vertical boresight polarization possible depending on which segments are moved. For the case where all four segments of the main reflector are translated and rotated in a prescribed manner, circular polarization on boresight results, with either right-

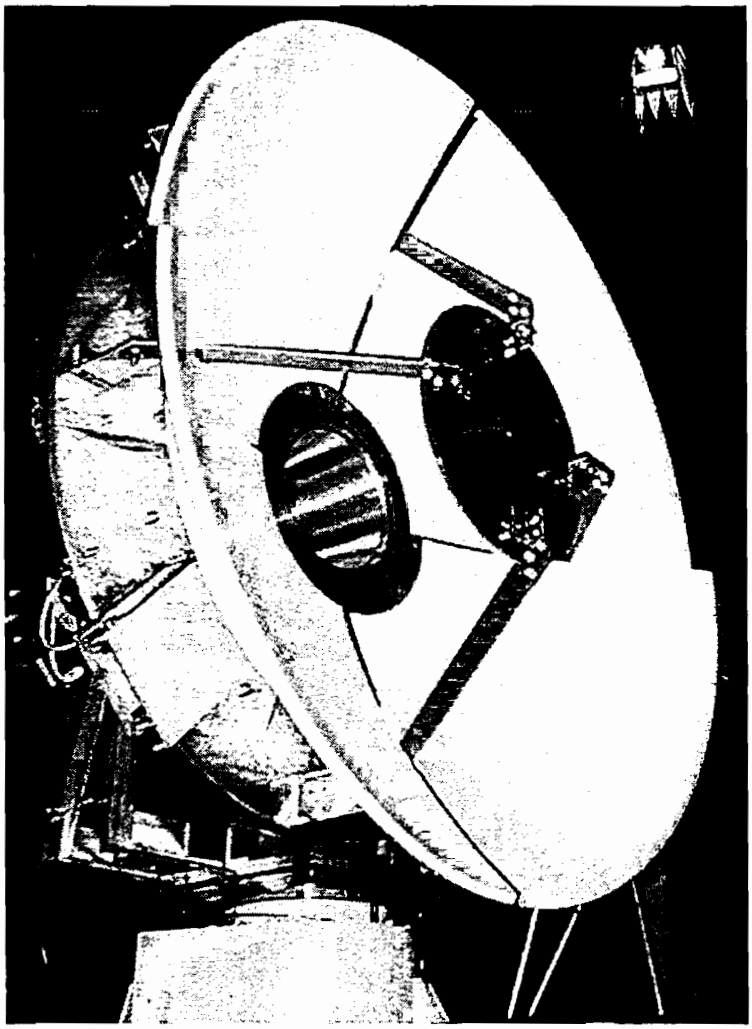

Figure 1. **The Cassegrain-type, Coaxial Beam-Rotating Antenna (COBRA) is shown mounted on an azimuth positioner. The segments of the COBRA II are positioned to yield circular polarization on boresight.**

hand circular polarization (RHCP) or left-hand circular polarization (LHCP) on boresight possible depending on the relative placement of the segments.

The positioning of each of the four segments of the main reflector was accomplished though the coordinated action of an array of four identical positioning systems. A scissors jack assembly, linear actuator, actuator controller, personal computer and custom software comprised each segment's positioning system. The asymmetric scissors jack assembly allowed the system to apply the correct translation and rotation of each segment through only a translational motion provided by a linear actuator. The automated nature of the positioning system allowed quick and accurate reconfiguration of the positions of the four segments of the main reflector, and permitted the rapid adjustment of the boresight radiated field from horizontal, vertical, RHCP or LHCP. To verify the placement of the main reflector segments and to calibrate the automated positioning

system, a unique measurement system was designed and built. It permitted the accurate determination (fractions of a wavelength $\approx \lambda/50$) of the relative positions of points on each segment surface as functions of azimuth, radial distance, and position along an arc from the vertex of the parabola to the outer rim. The third section of this note describes in detail the physical dimensions of the major components and subsystems of the COBRA II, its positioning system, and the measurement and position verification techniques.

Detailed measurements of the operating characteristics of the COBRA II were made over the 2.6 – 4.0 GHz band at both the High Energy Microwave Laboratory (HEML) and the Large Electromagnetic System Level Illuminator (LESLI) facilities. These included measurements of the radiated patterns and absolute gain of the feed horn, and all possible configurations of the four segments of the main reflector. The input impedance of the antenna was measured. Also, when the antenna was configured to produce circular polarization on boresight, the relative phase relationship of the two linear components was measured. Data representative of these measurements is presented in Section Four.

Finally, Section Five provides an overview of the COBRA II physical parameters and a summary of the operating characteristics. This includes calculations of the aperture efficiency and concluding discussion of other aspects of the antenna and its measured performance.

2. System Concept

This section briefly describes the fundamental concepts associated with a Cassegrain antenna system. Next, the applications of these principles to the COBRA II system are mentioned. After these motivating remarks, the scheme to accomplish the required segment positioning is explained, including the approximations needed to realize a practical system. Finally, a small section on aperture mode conversion is given.

2.1 Fundamental Principals

The basic concepts and the fundamentals of operation of the Coaxial Beam-Rotating Antenna (COBRA) have been described in previous papers and presentations [Ref. 7, 8, and 9]. Briefly, COBRA-type antenna systems use relative placement of reflecting surfaces to modify various path lengths from the focal point to the aperture plane to achieve an aperture distribution that produces the desired radiation pattern. In this case, the COBRA II prototype uses a Cassegrain system with a main reflector, subreflector and feed horn.

In a typical Cassegrain system, the focus of the primary reflector is coincident with the focus of the hyperbolic surface of the subreflector. The conjugate focus of the subreflector is typically located at the focus of the feed point. All rays that emanate from the feed point appear, after reflection from the surface of the subreflector, to have originated from the focal point of the parabolic main reflector. Figure 2 illustrates the geometry.

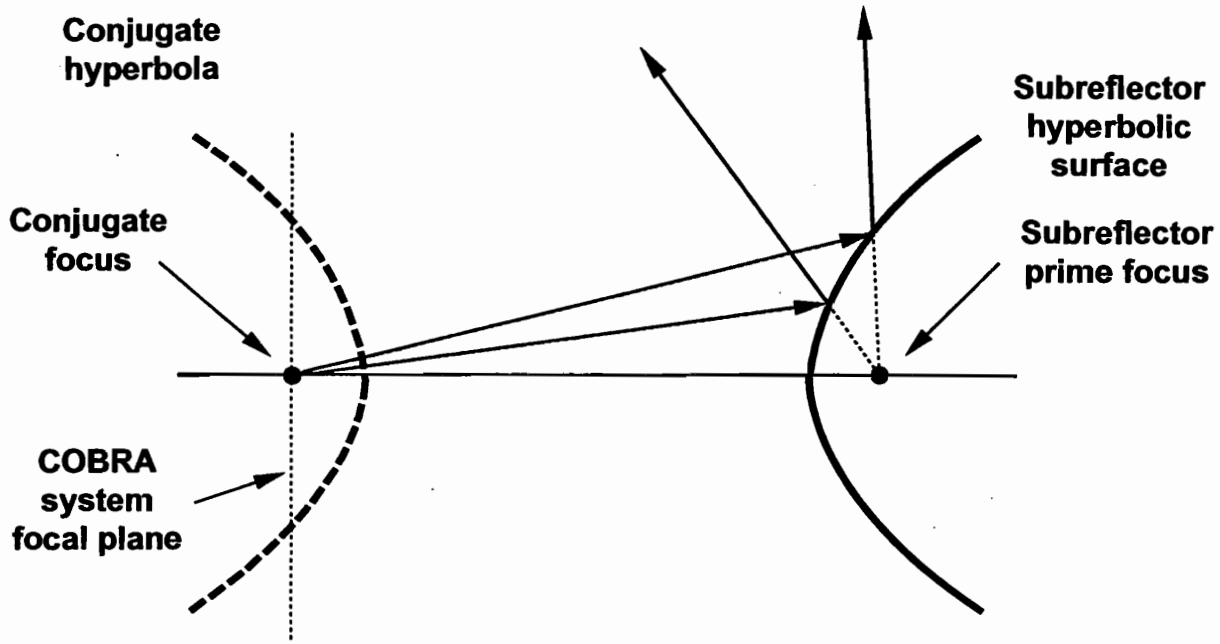

Figure 2. **Rays originating from the subreflector conjugate focus, that are reflected off the subreflector, are optically equivalent to rays from the subreflector's prime focus.**

To achieve the required aperture distribution, the COBRA II main reflector has been partitioned into four equivalent sectors or petals. Figure 3 shows a schematic of the four-segment (petal), Cassegrain COBRA. A cross sectional view of each petal is shown so that the path length differences can be illustrated. As in the figure, each segment is displaced from its neighbor (through a combination of rotation and translation) such that the path length from the phase center of the feed horn to the aperture plane differs by $\lambda/4$ for adjacent segments.

In this case the path length differences are obtained by movement (a combination of translation and rotation) of the petals comprising the main reflector. However this path length difference could be achieved by other methods. These include modifying the surface of the subreflector, or proper lensing of the feed horn.

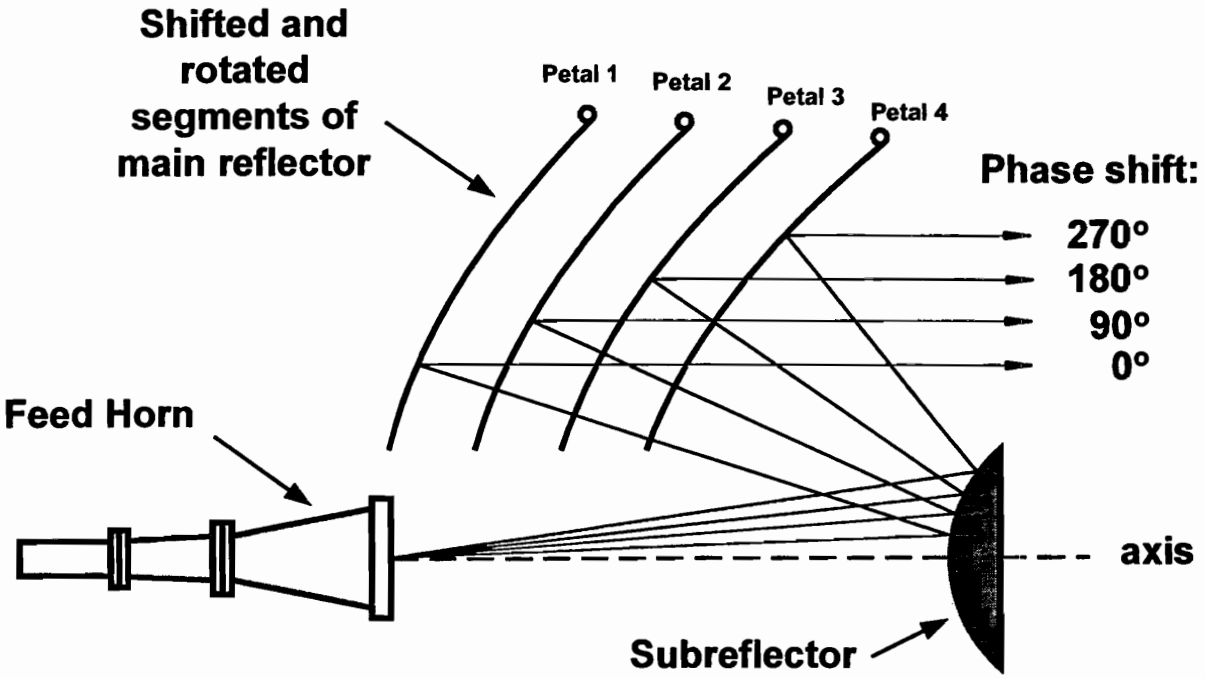

Figure 3. **A schematic of the four-segment (petal), Cassegrain COBRA. Each segment is displaced from its neighbor, through a combination of rotation and translation, such that the path length from the phase center of the feed horn to the aperture plane differs by $\lambda/4$ for adjacent segments.**

3. Segment Positioning and System Approximations

The different profiles of the four sectors of the main reflector would ordinarily dictate four different sector profiles with four different focal lengths. This would be impractical. We instead use the four sectors of the main reflector and approximate the desired profile through a combination of sector translation and rotation. From [Ref. 7] the required segment profile to realize the desired modification to the aperture field is given by

$$\tau_n(\theta) = \frac{(n-1)\lambda}{N(1+\cos\theta)} \tag{3.1}$$

For the specific circumstances associated with the COBRA II, $f = 3$ GHz and $N = 4$, the displacement of the contour of each sector can be computed as a function of the angle from the axis of the antenna. Figure 4a shows pictorially the displacement from nominal of a petal as a function of angle. In Figure 4b is shown the displacement from the nominal contour for each of the four segments as a function of the angle from the axis of the antenna. One can note that the displacement required is not a simple linear translation. In fact, according to Equation 3.1, each petal takes the contour of a new parabola with the same focal point (but different focal lengths) as the original, or nominal, parabola.

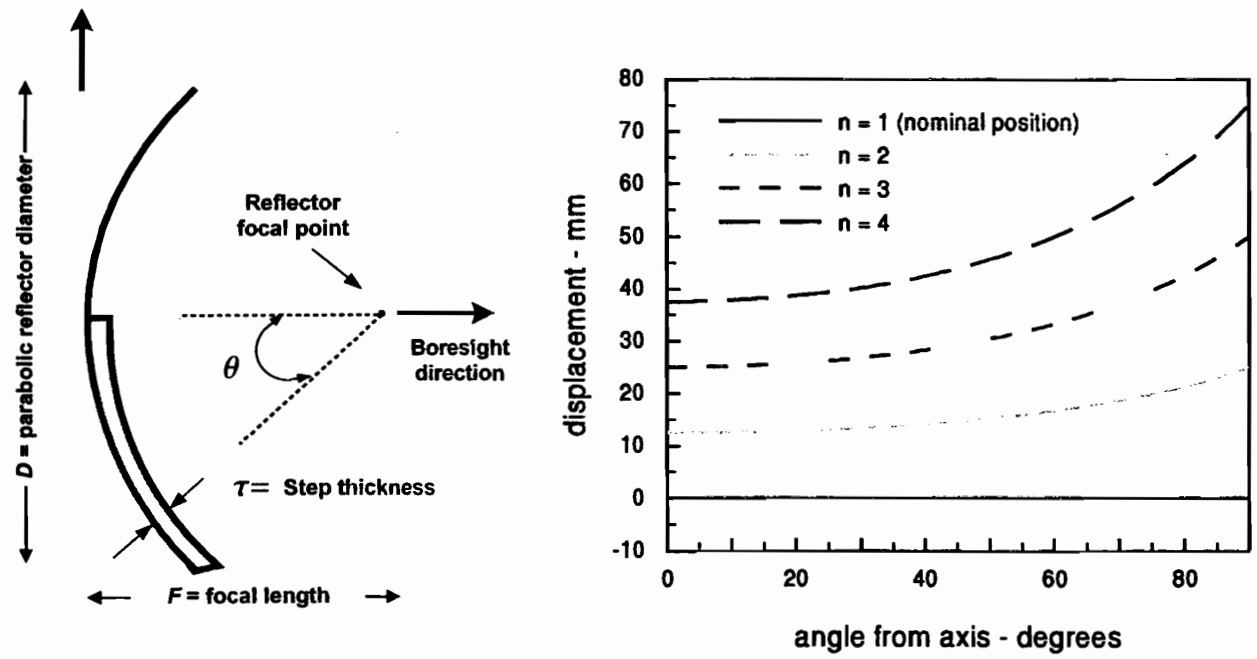

Figure 4. The COBRA II achieves the desired radiation property by adjusting the locations of the four petals: (a) the geometry; and (b) the displacement from its nominal position of each of the four petals.

In addition, since each segment must focus at the same point, a single (unique) subreflector profile is absolutely correct for each of the four main reflector segments of the COBRA II Cassegrain system. This is a consequence of the property that a hyperbolic surface reflects rays (emanating from the conjugate focus) such that they appear to originate from a point source at the prime focus of the hyperbola. Fortunately four different subreflector profiles are not required. The ability to accurately position each of the four sectors of the main reflecting surface to approximate the "true" contour is described later in this note.

3.1 Mode Conversion

The modification of the aperture field distribution to achieve the desired boresight properties is accomplished though the path length differences induced by the relative displacement of the main reflector petals from one another. The path length difference (Δl) relates directly to a phase shift ($\Delta\phi$) as

$$\Delta\phi = \frac{2\pi}{\lambda}\Delta l = \frac{2\pi}{\lambda}(n-1)\frac{\lambda}{4} = \frac{\pi}{2}(n-1) \tag{3.2}$$

where $n = 1, 2, 3$ or 4. As explained, the function of the re-positioned segments of the main reflector is to transform an azimuthally symmetric aperture distribution, which would normally

produce a boresight null, into a distribution that produces a boresight peak. The azimuthally symmetric aperture distribution can be written as

$$\mathbf{E}(\rho,\phi) = E(\rho)\,\hat{\mathbf{u}}_\rho . \tag{3.3}$$

The effect of the path length differences on the aperture field distribution (ignoring the slight effect on magnitude) is then

$$\mathbf{E}(\rho,\phi) = E(\rho)\,\hat{\mathbf{u}}_\rho \times e^{-j\frac{2\pi}{\lambda}\Delta l} = E(\rho)\,\hat{\mathbf{u}}_\rho \times e^{-j\frac{\pi}{2}(n-1)} . \tag{3.4}$$

This effect can be illustrated graphically as follows. From (3.3) the $x-$component of the unmodified aperture field in the time domain is

$$E_x(\rho,\phi,t) = \mathrm{Re}\left[\mathbf{E}(\rho,\phi)\cdot\hat{\mathbf{u}}_x \times e^{j\omega t}\right] = \mathrm{Re}\left[E(\rho)\,\hat{\mathbf{u}}_\rho \cdot \hat{\mathbf{u}}_x \times e^{j\omega t}\right] = \mathrm{Re}\left[E(\rho)\cos(\phi)\times e^{j\omega t}\right]. \tag{3.5}$$

For $t = 0$, the normalized value of the electric field (plotted for an arbitrary value of ρ) is shown in Figure 5a, plotted over the azimuth interval $(0,2\pi)$. If integrated in azimuth over the same interval, (3.5) yields a value of 0 for all values of time *t*, which is another way of saying that the boresight electric field is zero as well. In contrast, from (3.4) the $x-$component of the unmodified aperture field in the time domain is

$$E_x(\rho,\phi,t) = \mathrm{Re}\left[\mathbf{E}(\rho,\phi)\cdot\hat{\mathbf{u}}_x \times e^{-j\frac{\pi}{2}(n-1)} \times e^{j\omega t}\right] = \mathrm{Re}\left[E(\rho)\cos(\phi)\times e^{-j\frac{\pi}{2}(n-1)} \times e^{j\omega t}\right]. \tag{3.6}$$

For $t = 0$, the normalized value of the electric field is shown in Figure 5b, plotted over the azimuth interval $(0,2\pi)$. If this expression is integrated in azimuth over the same interval, a value other than 0 results (except for isolated values of time *t* that correspond to 0's of the *x*-component of the circularly polarized wave), which is another way of saying that the boresight electric field is non-zero. A plot of (3.6), for arbitrary value of ρ, for the time interval $t = (0,T)$, where T = period, is shown in Figure 6.

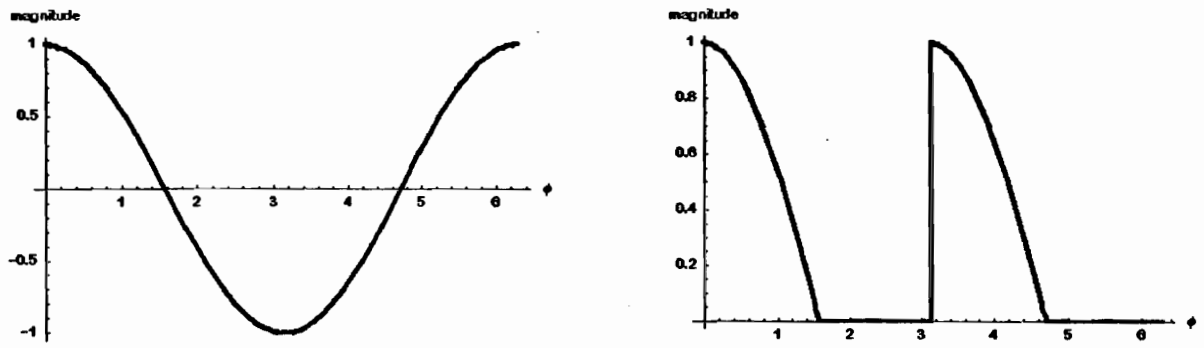

Figure 5. The normalized value of the aperture electric field at $t = 0$: (a) described by (3.5); and (3.6).

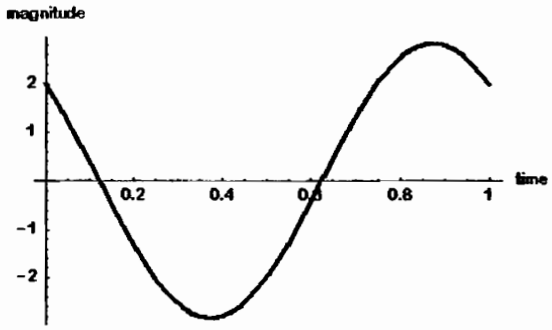

Figure 6. The integral of (3.6) over the interval $t = (0, T)$ for arbitrary value of ρ.

The above explains the manner in which the prescribed segment positioning scheme results in a modification of the aperture field. More detailed explanations of these fundamental concepts, derivations of governing equations, and performance predictions are to be found in [Ref. 7].

4. System Elements

The physical properties of the major elements and each sub-system of the COBRA II prototype are described in this section. This includes a description of the main reflector, subreflector, feed horn, sector positioning system, and profile measurement apparatus.

4.1 Main Reflector

The COBRA main reflector is fabricated of a spun metal parabolic reflector with a ratio of focal length to diameter of 0.26. This value of f/D ratio was chosen to minimize the total antenna volume (by making the focal point close in to the main reflector), it was also the f/D value of a readily obtained surplus reflector - the focal point of this reflector is approximately in the plane defined by the dish's rim. The main reflector diameter is about 68 inches, but the usable reflecting surface is only the inner 62.5 inches; the rest being a rolled rim that provides mechanical rigidity to the dish. The main reflector is depicted in Figure 7.

A circular hole was cut in the reflector to allow a conical feed horn to be placed at the parabola's vertex. The dish was also cut into four identical segments (quadrants) by removing an inch-wide strip from the dish along two perpendicular axes. This was done to ensure that the

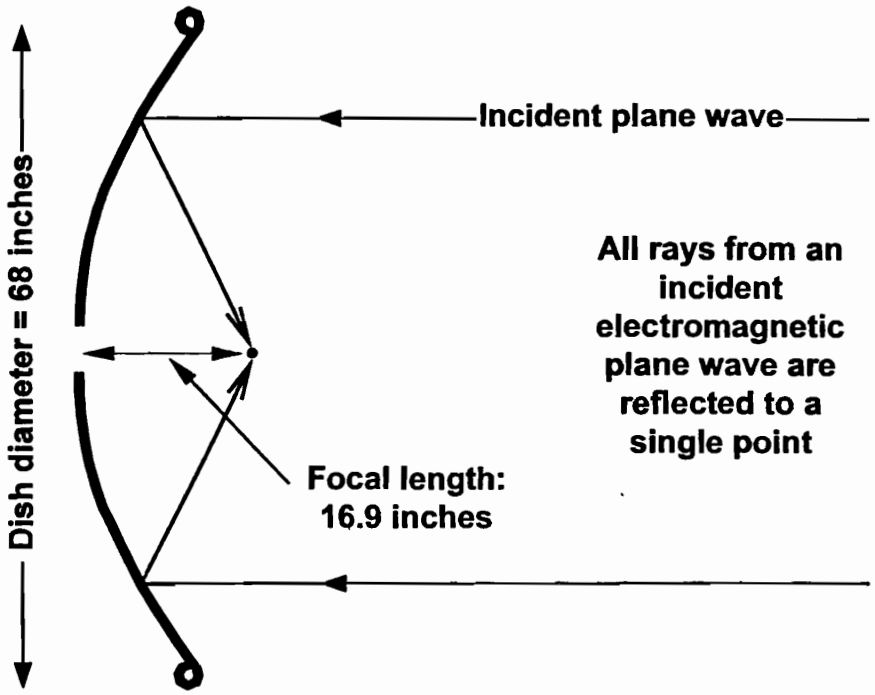

Figure 7. Main Parabolic Reflector.

reflector segments could be positioned without interfering with each other in any of the COBRA configurations. The segmented dish with the shifted segments is illustrated below in Figure 8a; the actual segments cut from the parabolic reflector are shown in Figure 8b.

4.2 Subreflector

The COBRA II prototype uses a hyperbolic subreflector whose prime focus is collocated at the focal point of the main parabolic reflector. The pair of reflecting surfaces acts like a single parabolic reflector, but with a different focal plane than that of the main reflector. The desired location of the system focal plane or feed point determines the required eccentricity of the subreflector. The focal plane is located at the conjugate focus of the subreflector, so the subreflector must be positioned with its prime focus at the focal point of the main parabolic reflector, and its conjugate focus located at the desired feed point of the conical horn. These constraints determine a unique eccentricity or surface shape for the subreflector.

The subreflector diameter is 21 inches, a little less than $^1/_3$ of the main reflector. This diameter is almost optimal for maximum efficiency (minimizing spill over, but optimally illuminating the outer extremes of the main reflector). Two major design parameters must be considered when selecting the subreflector size. There is a loss of efficiency due to the obstruction (shadowing) of the main reflector by the subreflector. Small subreflectors diminish loss of efficiency by subreflector shadowing. There is also a loss of efficiency caused by failure of the subreflector to intercept all of the energy radiated from the feed horn. The subreflector must be large enough to intercept most of the energy radiated by the feed horn. Maximum interception of feed horn radiation by the subreflector occurs with larger diameters. The loss of

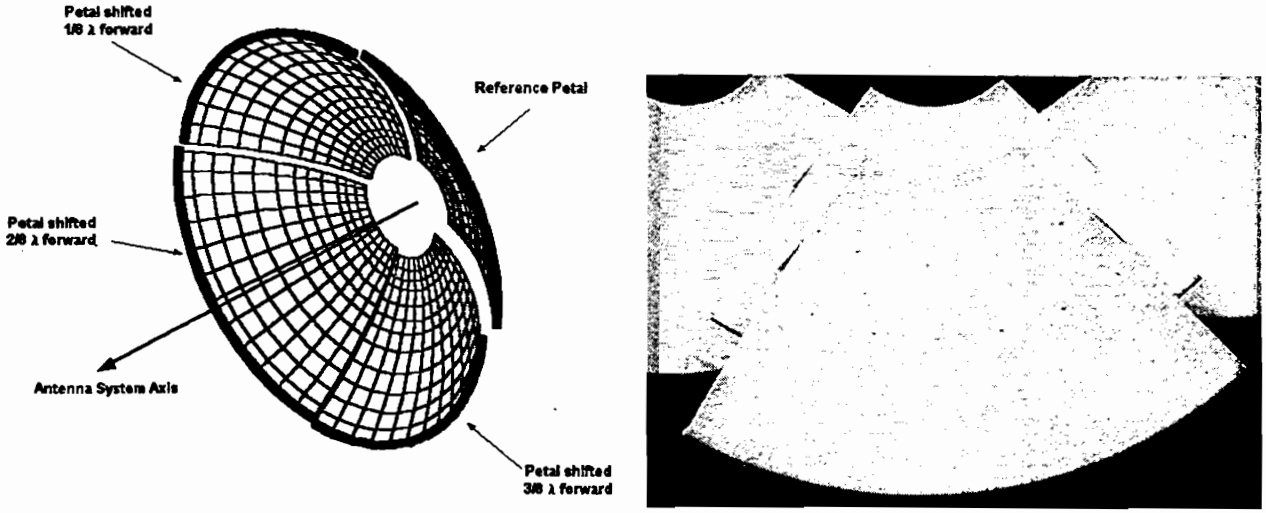

Figure 8. The man reflector: (a) schematic of the translated segments of the main parabolic reflector; and (b) the four petals.

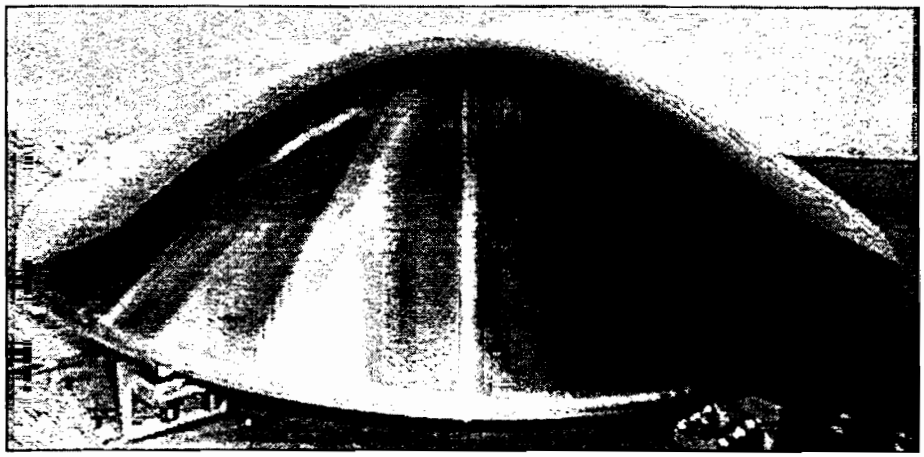

Figure 9. The COBRA II subreflector.

efficiency due to shadowing of the primary reflector, and non-intercepted feed horn radiation must be balanced by choosing a subreflector diameter that is near the minimum of the combined effects. For the feed horn diameter of 14 inches, and (useable) main reflector diameter of 62.5 inches, the 21-inch subreflector diameter was calculated to be an optimal size.

4.3 Feed horn

The focal plane/feed point for the COBRA system described here was designed to be at the vertex of the main parabolic reflector. Thus, when the aperture of the conical feed horn is placed at the main reflector's vertex, the system will focus divergent radiated power from the feed horn aperture into a narrow parallel beam.

The feed horn, shown in Figure 10, has three sections: a circular waveguide section, a tapered transition section, and a conical horn section. The circular waveguide section was fabricated with a coax-to-waveguide adapter at its input end. The adapter is basically a monopole stub which is oriented along the longitudinal axis of the circular waveguide, the adapter is positioned to launch a TM_{01} mode in the circular waveguide section of the feed horn assembly. The next section of the feed assembly is a transition section, which tapers the diameter from the 3.5 inches of the circular waveguide section to the beginning diameter of the conical horn. The last section is a conical horn that opens into a 14-inch circular aperture. The entire feed horn can be translated (moved) along the main axis (forward and backwards) of the antenna system to allow optimum positioning of the feed horn with respect to the subreflector.

4.4 Petal Positioning System

To achieve the correct aperture distribution the four individual segments (petals) of the main reflector must be positioned along the antenna system axis at different distances from the subreflector. The locations of the petals are quite specific. The nominal position of all petals is such that the focal length of each petal is collocated with the prime focus of the subreflector. Then, in order to minimize defocusing of a quadrant associated with a particular petal, the petals are then symmetrically displaced forwards and behind the nominal position. Then, to produce the desired boresight sight peak with circular polarization (from an azimuthally symmetric mode) the positioned such that a ray from the phase center of the feed horn, to the subreflector, to the surface of each petal and on to the antenna aperture plane would be $\pm\lambda/8$ and $\pm 3\lambda/8$ from the nominal (reference) position.

For the system to work, each petal must still approximately focus its reflected energy to the location of the reference position's focal point. To do this, each petal should have a different focal length, but

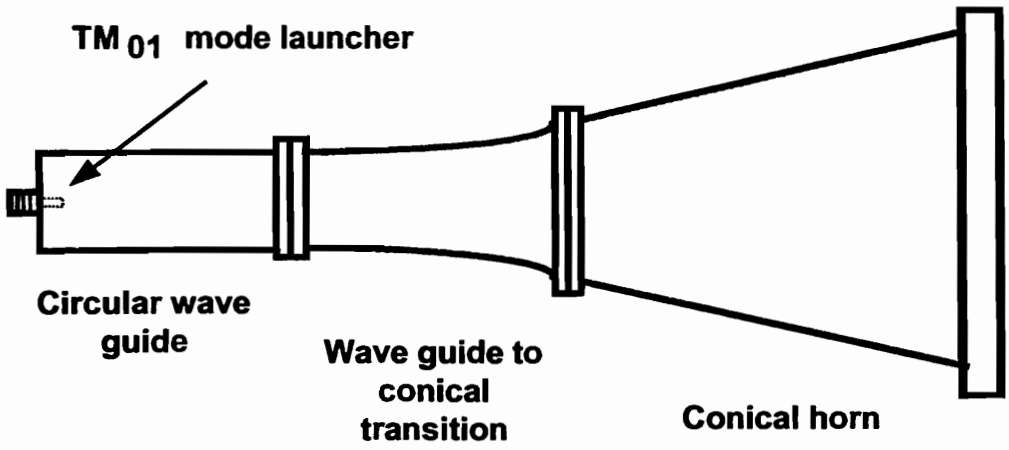

Figure 10. Conical Feed Horn

since they were cut from the same parabolic reflector, each petal has the same focal length as the original reflector. A method of changing the effective focal length of each petal was devised. If the petals are rotated inward towards the system axis, much of the petals' surface can be made to closely coincide with an ideal reflecting surface with a shorter focal length. The necessary rotation, corresponding to each petal position, was accomplished by mounting the petals on an unequal arm scissors jack assembly. The unequal arm jack was designed to provide the correct rotation for all translated positions of the petals. Thus, the need for different focal length petals is eliminated and the effective focal length of each petal could then be shortened by an appropriate rotation.

4.4.1 Asymmetric Scissors Jack

The petal positioning system of the COBRA II comprises four principal constituents. These included: the asymmetric scissors jacks that provided a combination of translation and rotation to each petal; the linear actuators that were used to drive precisely the scissors jack assemblies; the linear actuator controllers; and the COBRA II system computer and software. Each of these elements of the petal position control system is described below.

The scissors jack assemblies were designed to provide the relocation required by the petals to accurately mimic the different focal lengths required. This motion consists of a precise linear translation as well as a measured angle of rotation. In this design, the asymmetry in the jack was 10 inches $\times$ 12.15 inches, which provides a rotation of 1.36° for every inch of petal translation. The scissors jack provides almost linear performance in the small usable range in the flat portion of the curve. The more vertically the jack extends, the more non-linear its performance becomes. Figure 11 shows the rotation (degrees) undergone by the petal as a function of the translation of the scissors jack assembly. It can be seen that the angle of rotation is 90° at 12.15 inches of translation, which corresponds to the full extension of the jack. The non-linear performance is easily seen, and the usable portion of the mechanism, which well approximates a linear relationship, is indicated. Figure 12 shows an expanded view of the difference (error) between the ideal (desired) and actual performance of the jack assembly. Also indicated in the figure are the limits of $\pm \lambda / 30$ as error bars.

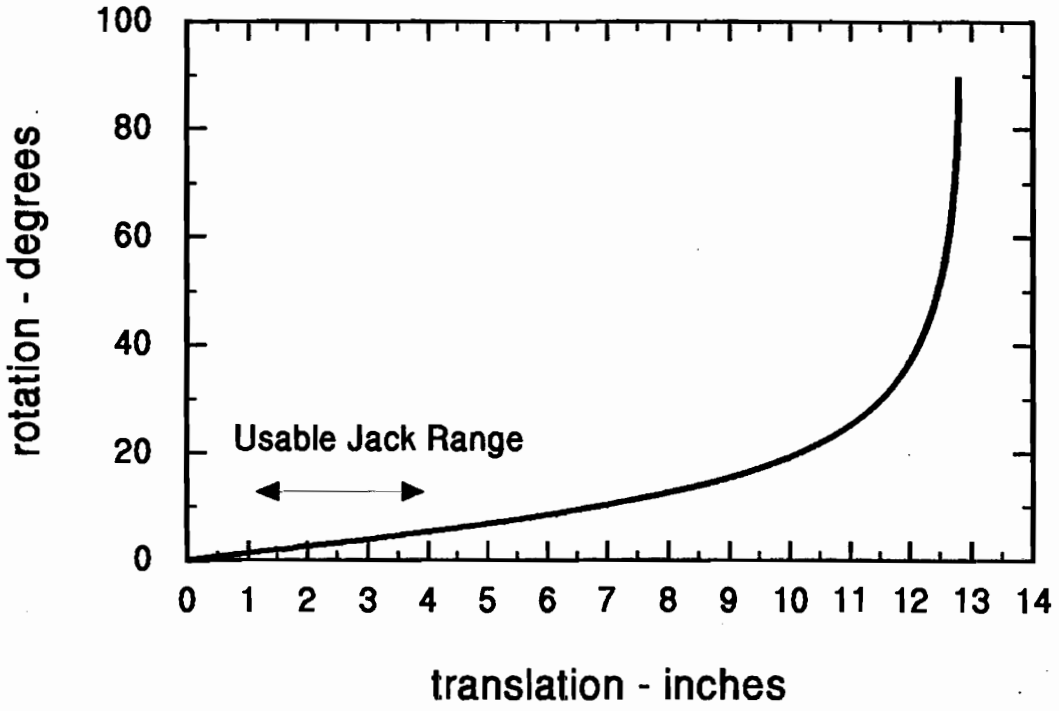

Figure 11. Scissors jack translation vs. rotation.

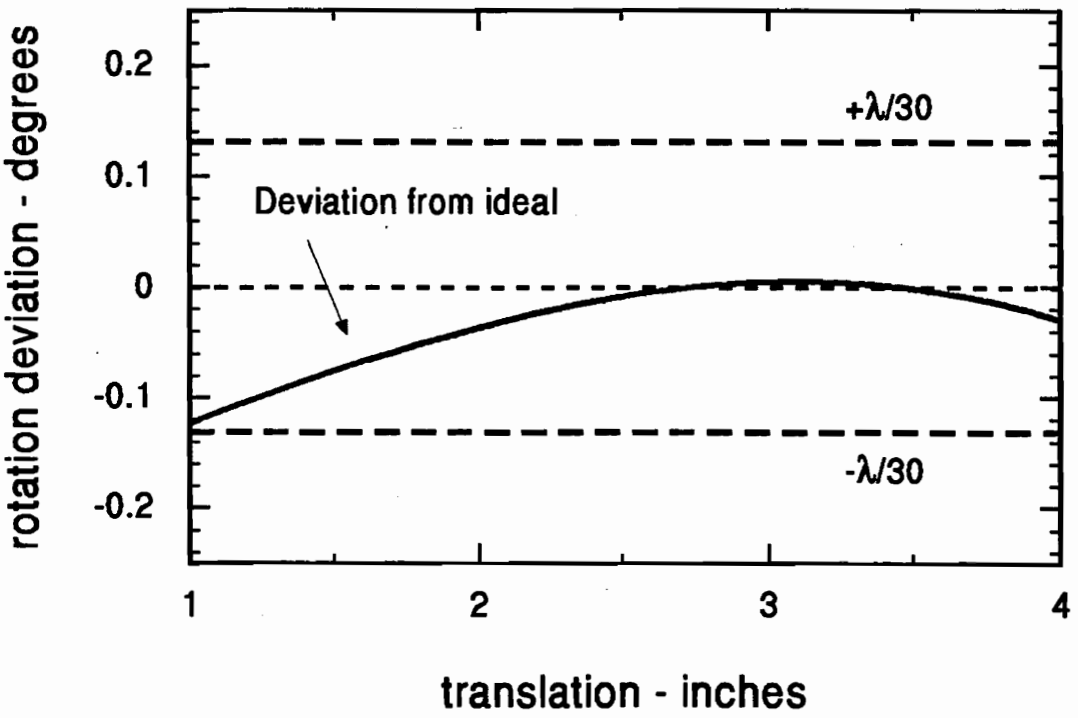

Figure 12. Scissors jack rotation error vs. translation

Figure 13 shows the major components of the Asymmetric Scissors Jack assembly. The turnbuckle adjusts the translation vs. rotation ratio by changing the length of the asymmetric arm. A longer arm provides more rotation for a given translation drive, and less rotation for a shorter arm length. The turnbuckle has both right and left-handed threads to allow infinite variation within the adjustment range. The ball joint and adjustment screws allow for two-dimensional rotational adjustment of the main reflector segment attached to the jack. This provides for precise rotational alignment at a given jack translation position. The sliding joints allow the jack assembly to extend and contract without binding, and yet vertical play is minimal so that positioning is very repeatable. These sliding joints also allow the drive attachment to move linearly, as is required by the linear actuator. The drive attachment is the connection point from the scissors jack to the linear actuator drive.

4.4.2 Linear Actuator

The linear actuators are linear-drive, stepper-motor devices used to provide the automated control of the jack position. Each unit has a 4-inch total travel with 1,000 steps per linear inch of drive. These actuators will apply up to 135 lb. of force on the jack assembly, which exceeds the real force required to properly position the reflector segments. Each actuator has three Hall effect sensors mounted on the actuator body to provide the required sensing: forward limit, rear limit, and "Home" reference. These sensors are connected directly to the actuator controller as feedback.

4.4.3 Actuator Controller

The actuator controllers are programmable, microprocessor-controlled, stepper-motor amplifiers used to provide monitoring and control of the linear actuators. Each actuator has its own

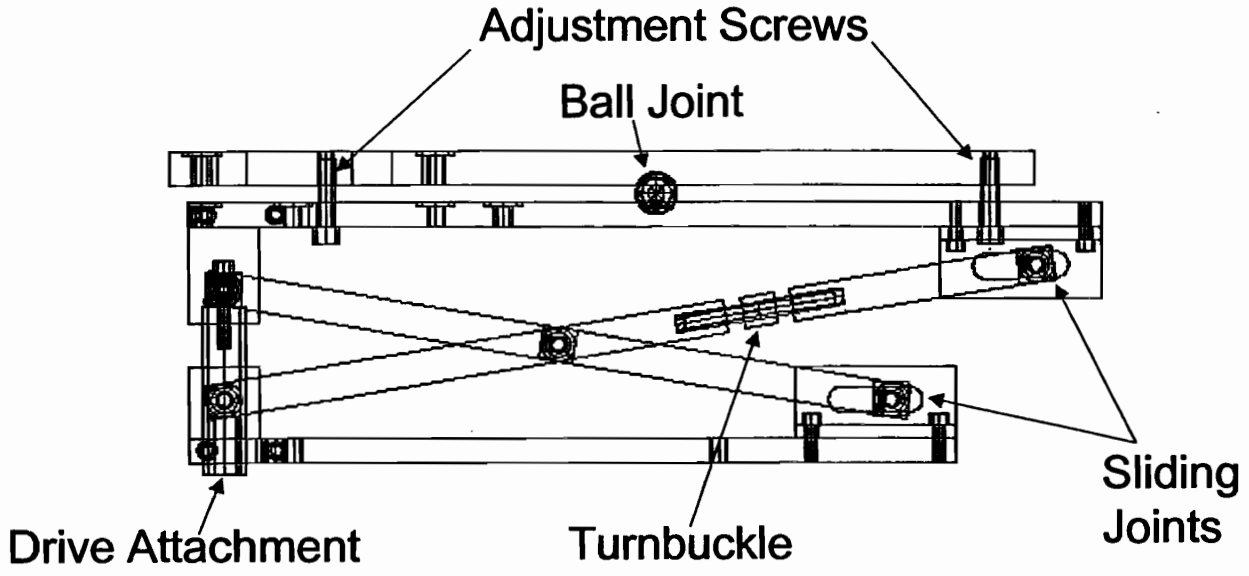

Figure 13. Side view of an asymmetric scissors jack.

controller and is individually programmed via RS-232 from a remote computer, or through the factory supplied plug-in keypad that allows the user to program the controller through a series of menu items. These controllers have been programmed for acceleration rate, deceleration rate, maximum velocity, and limit sensing, among many other parameters. The controller is also programmed to seek the "Home" position and set the counters to zero as an absolute position reference. This reference has been found to be repeatable to much less than ±0.005 inches.

4.4.4 System Computer

The system computer is an Intel 486-based laptop running Windows 95. This computer connects to the four actuators via a daisy-chained RS-232 link to its Serial 1 port. From there, a simple command line program is run that automatically initializes the actuators, then commands them all to move to a preset position unique to each actuator. Presently, that position is set at Position 1 for each of the four systems, although it is simple to change that to any position by editing a small text file. After initialization, a command prompts the user to enter a command to move any of the four actuators.

The COBRA motion control system was calibrated using the measurement system described later in this report, and each reflector segment has its effective focal lengths and actuator position information correlated in a table corresponding to the ideal positions for operation at a frequency of 3.0 GHz. This information is used to set the segment positions for a variety of configurations by entering the desired position information in the command line and instructing the controllers to move to the new positions. In this way all positioning is automated, allowing the COBRA II to be repositioned in a matter of two or three minutes, instead of the hours required to reposition the COBRA I prototype.

4.5 Surface Profile Measurement and Verification Apparatus

For the COBRA system to work properly, a means to calibrate and verify the position and orientation of the main reflector surfaces was required. For the first COBRA prototype, a circular track was made that held a cylindrical measurement system that measured θ (angle of rotation), r (radial distance), and d (depth). This system was somewhat difficult due to its relatively poor reproducibility of measurements. There was play in the tracks, as well as play in the ball wheels that lay in the tracks. Another difficulty was that the depth measurement required the operator to maintain perpendicularity to the measurement fixture, which compounded the reproducibility problem.

For the COBRA II prototype, a new measurement system was designed yield more reproducible and accurate measurements, as well as easier to use. This system uses a pseudo-spherical coordinate system to measure θ (angle of rotation), ϕ (angle of elevation) and r (radial length). The system, shown in Figure 14, is more stable and repeatable than the previous system because it uses a pivotable post rather than a large wide structure riding on a track.

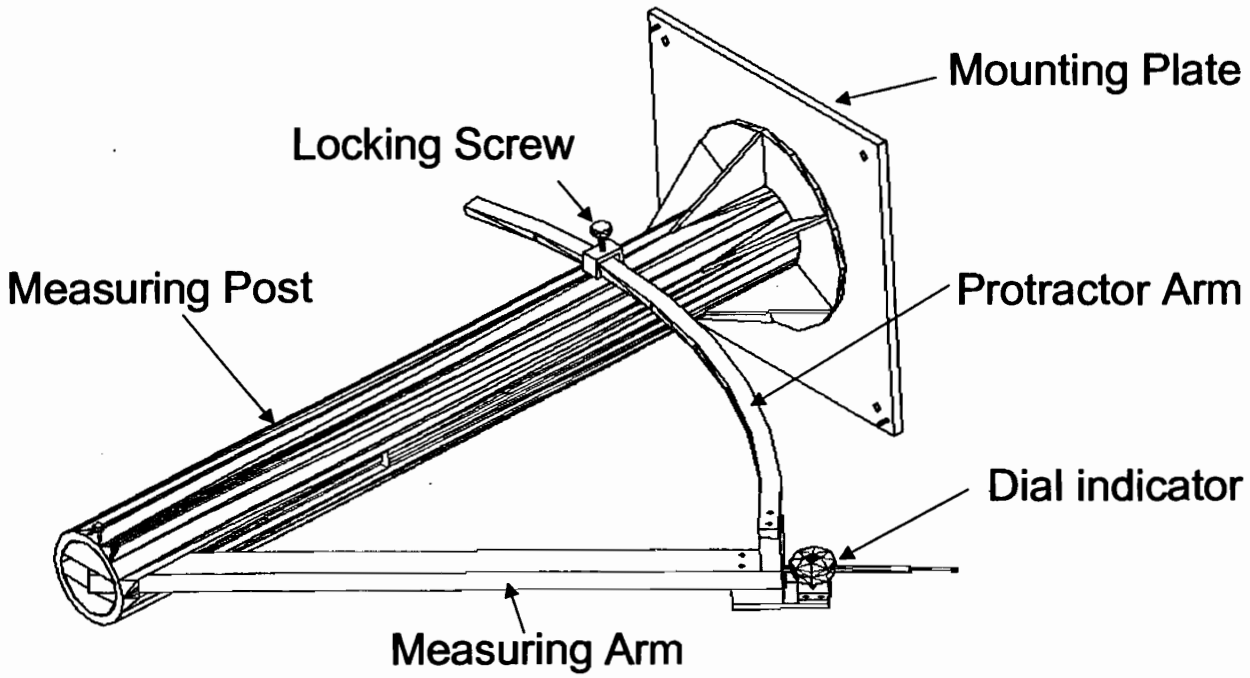

Figure 14 Measuring Post and Major Components.

As shown in Figure 14, the measurement system is fastened to a mounting plate, which is bolted in the center hole of the COBRA main mounting plate (see Figure 15). This plate is used as the absolute reference for the COBRA measurement system, all measurements are made relative to it. The mounting plate is pinned so that it can be mounted onto the main plate in only one way. It should be noted here that the measuring system can be attached only when the feed horn and the subreflector are removed. The measuring post is then bolted to the mounting plate with a ¾ inch – No. 10 bolt. The reinforced bottom of the post is ground flat to ensure that the measuring post is perpendicular to the ground face of the mounting plate when tightened with the ¾ inch bolt. The angle, ϕ, is set by loosening the ¾ inch bolt and allowing the entire assembly to pivot around the bolt so that the operator may set the system at a specific angle. The graduations are printed on the mounting plate and are in 1.0° steps, and measurement repeatability is greater than 0.25°.

The measuring post is 5.0 inches in diameter, made of ½-inch thick aluminum tubing, and is 44.675 inches long to provide maximum stiffness and minimize any sagging effects. The measurement arm is connected to the measuring post at its end via a bolted pivot joint. This joint is designed for minimal play with ease of rotational movement of the measurement arm. The measurement arm holds a dial indicator, which measures up to 4.0 inches of depth in 0.001-inch increments. Radial length (r) is determined by subtracting the depth measurement of the dial indicator from the fully combined length of the measurement arm and the fully extended dial indicator.

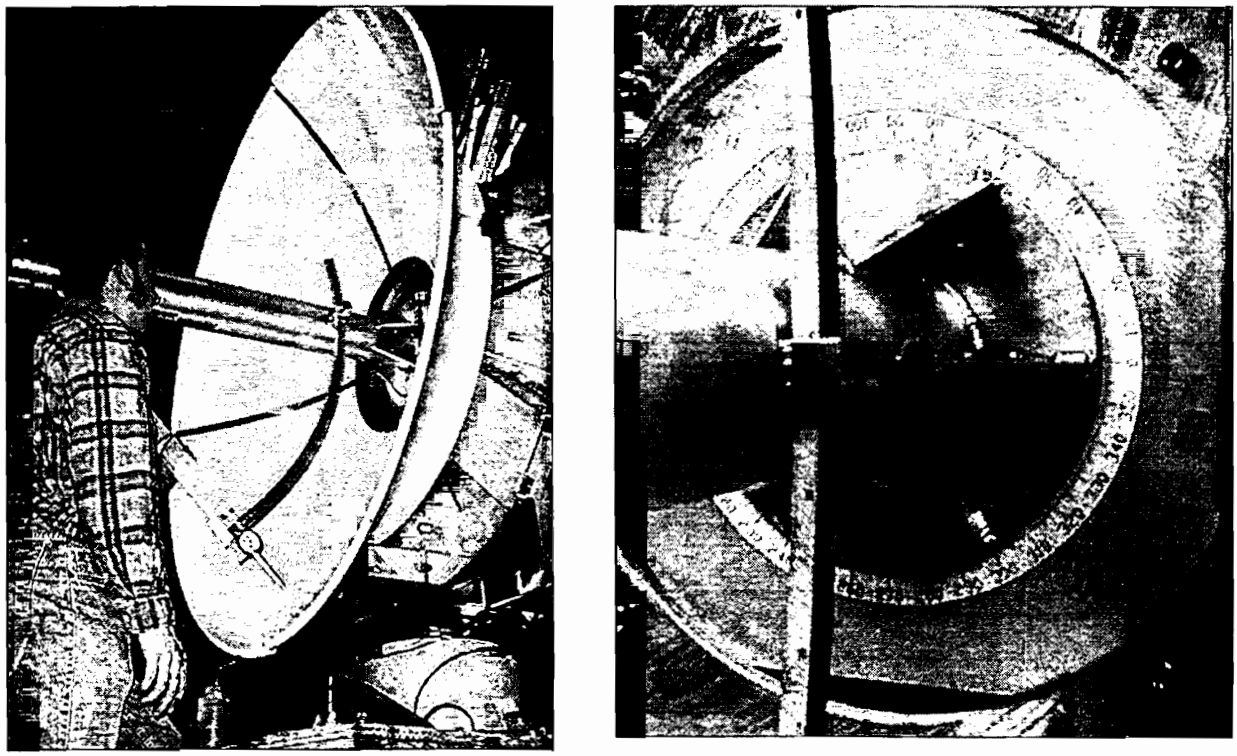

Figure 15. The contour measurement and verification apparatus shown mounted on the COBRA II.

Attached to the measurement arm is the protractor arm, which is an arc-shaped bar of rectangular aluminum. The protractor arm is used to set θ by the graduated marks printed on its upper surface. These marks are graduated in 0.1° steps and are easily readable at the long radius from the measurement arm pivot point. Measurement repeatability on this axis is much better than 0.05°. The locking screw holds the protractor arm at a specific angle (set by the operator) and holds the measurement arm assembly in place while the dial indicator depth measurements are made.

The nominal focal length of the main reflector is 16.875 inches. An equation was derived that related the radial value read by the measurement system, $R(\theta)$, as a function of the elevation angle θ,

$$R(\theta) = \frac{2}{\sin^2(\theta)} FL \left[\sqrt{\frac{\cos^2(\theta) FL + \sin^2(\theta) L_{post} - \sin^2(\theta) h}{FL}} - \cos(\theta) \right] \tag{4.1}$$

where $FL = 16.875$ inches, and $L_{post} = 42.852$ inches is the height of the post less the offset at the top (pivot point is not at the top of the post). A measurement of one of the petals in the nominal position (no displacement) was made, and the measured values of R are shown in Figure 16. Also, the values of R that would relate to a focal length of $FL = 16.875$ were determined.

These values are plotted in Figure 16 as well. One notes good agreement among the data, indicating good petal positioning.

The data plotted in Figure 16 are indicative of the alignment, but another way to view the alignment is to compute the effective focal length of each measurement. The effective focal length is the focal length value associated with a given measured $R(\theta)$, essentially solving Equation 4.1 for the focal length given the measured value of R. These data are shown in Figure 17, and indicate that the petal position (held and positioned by the petal jack assemblies) is in good alignment with the ideal.

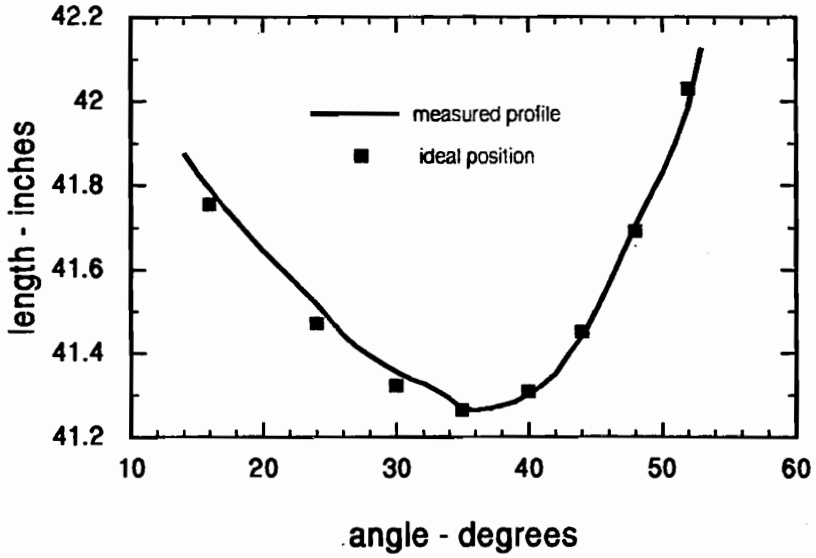

Figure 16. The measured and ideal values of the surface profile.

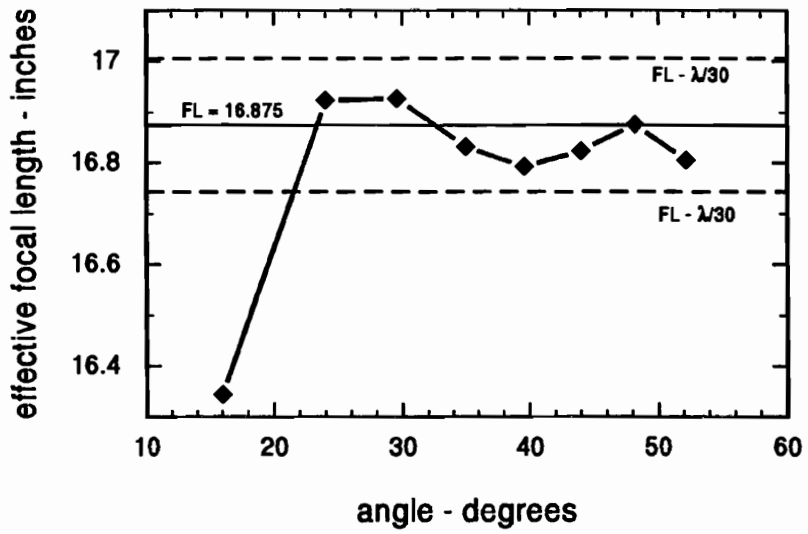

Figure 17. The effective focal length found by solving Equation 4.1 for the focal length as a function of measured $R(\theta)$.

5. Measured Performance Data

Measurements of the radiating properties of the COBRA II were conducted at the High Energy Microwave Laboratory (HEML) and the Large Electromagnetic System Level Illuminator (LESLI) facilities. The measurements were begun in the HEML facility, but the results were suspect since standard farfield separation distances could not be attained there. The $2D^2/\lambda$ farfield for the COBRA II prototype is approximately

$$2D^2/\lambda = 2\frac{(67\,in \times 2.54/100)^2}{0.1} \approx 58 \text{ meters} \qquad (5.1)$$

and the maximum separation available in the HEML chamber is about 20 meters. Consequently, the measurements of the farfield performance were suspect due to the nearfield nature of the measurement. To obtain true farfield results, we also conducted a true farfield, open-air test at the LESLI facility. After the results of both measurements were completed, we could see that the HEML measurements had yielded sufficiently accurate indications of the farfield performance of the COBRA II antenna; however, a great deal more data were gathered at the LESLI facility. The results presented below were gathered at both facilities. Where measurements of the same parameter were made at both facilities, the better and/or more reliable data are presented.

5.1 Feed Horn and COBRA II Input Impedance

The input impedance of the COBRA II feed horn was measured and is shown in Figure 18. The waveguide cutoff condition is easily identified, as well as a feed resonance condition. The nominal SWR across the operating band of the feed horn is approximately 1.5:1. The impedance mismatch results in reflection and loss of some of the power delivered to the terminals of the feed horn. The loss of power due to impedance mismatch is shown in Figure 19, and the nominal value of lost power is approximately –0.25 dB.

The impedance characteristic of the COBRA II is taken to be that of the feed horn. The only direct measurement of the COBRA II input impedance (feed horn mounted) was made at 3 GHz. The measured value of input impedance of the COBRA II at 3 GHz was

$$Z_{in}(3\,GHz) = 78.5 - j6\ \Omega\ ,$$

which results in a standing wave ratio of SWR = 1.6, as opposed to the measured value of the feed horn alone (SWR = 1.47).

In the data relating to antenna gain presented in the following sections, the values have **NOT** been adjusted for the power loss due to impedance mismatch. However, these effects are considered in the summary section.

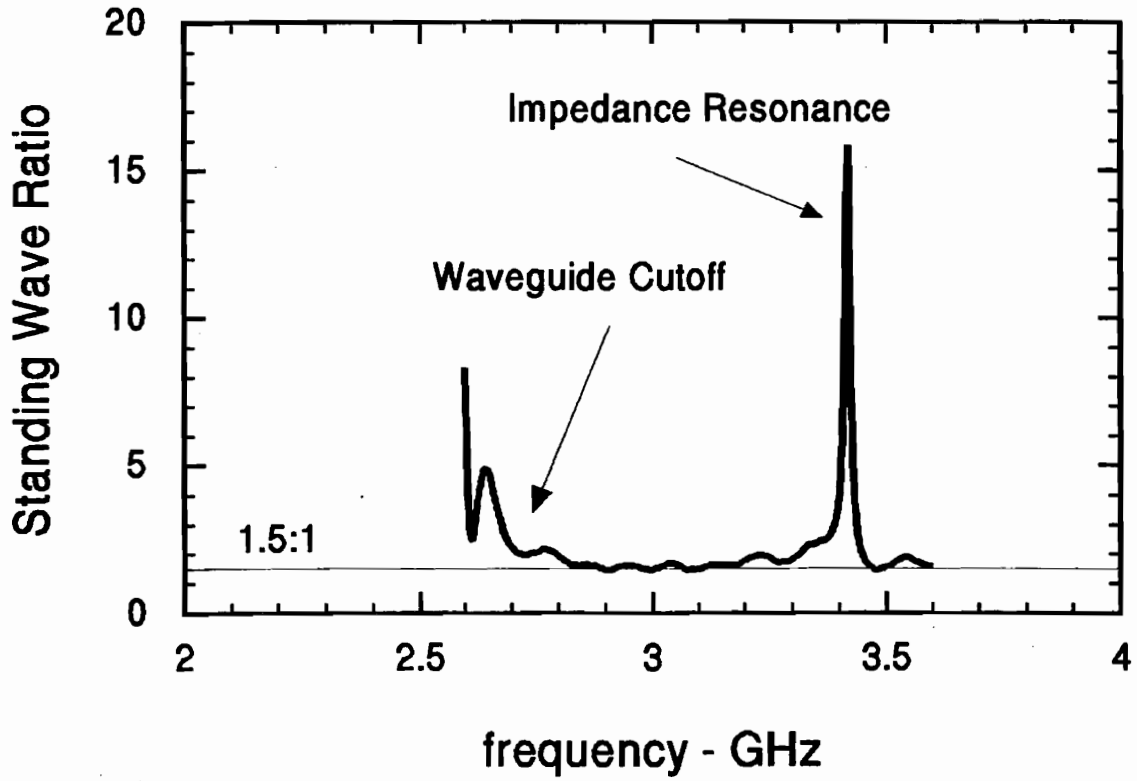

Figure 18. **The measured standing wave ratio at the input terminal of the feed horn.**

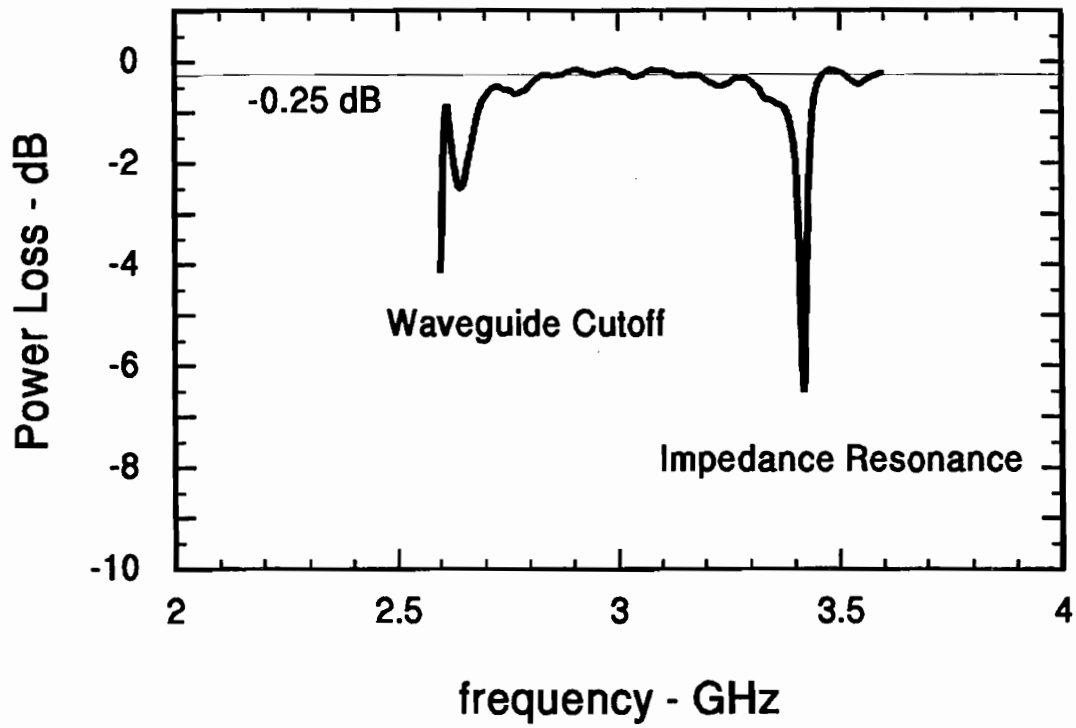

Figure 19. **The power loss due to impedance mismatch of the COBRA II feed horn.**

5.2 *Feed horn Pattern and Radiation Characteristics*

The geometry of the feed horn is described in detail in a previous section, but briefly the feed horn is approximately 4 feet in length with an aperture diameter = 14 inches. The TM_{01} mode is excited in the 3.5 inch diameter circular wave guide feed by a custom coaxial to circular waveguide transition. The azimuthal pattern, measured at 3 GHz, of the horizontal component of the radiated field of the feed horn is shown in Figure 20. The characteristic null on boresight is seen, and the peak pattern gain is shown to be about 13.5 dBi. The pattern peak occurs at about 12.5°, which agrees well with the standard formula [Ref. 10] for the pattern peak of a TM_{01} mode driven circular aperture

$$\phi_{peak} = \sin^{-1}\frac{0.382\lambda}{a} = \sin^{-1}\frac{0.382(0.1)}{0.1778} = \sin^{-1} 0.21485 = 12.41^{o}. \tag{5.2}$$

The peak pattern gain as a function of frequency was also measured. Figure 21 shows the peak pattern gain of the COBRA II feed horn over the frequency range of 2 – 4 GHz. The gain climbs rapidly above waveguide cutoff of

$$f_c = \frac{x_{np}}{2\pi a\sqrt{\varepsilon\mu}} = \frac{2.405}{2\pi(0.04445)}\left(2.998\times10^{8}\right) = 2.58\,\text{GHz} \tag{5.3}$$

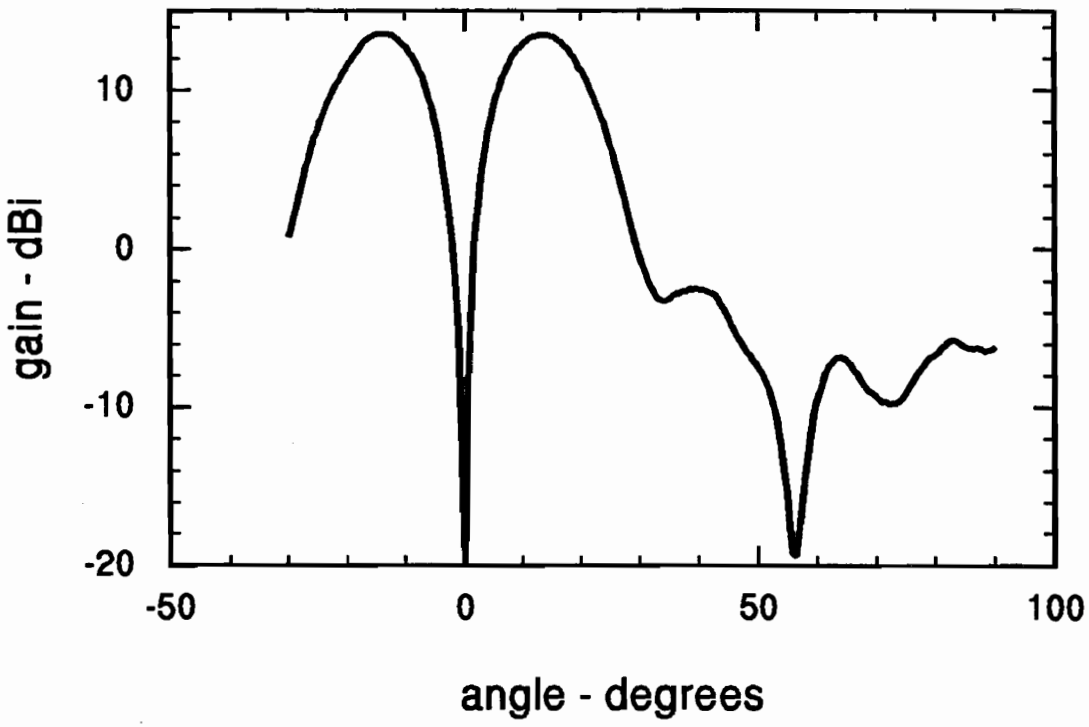

Figure 20. Azimuthal pattern, measured at 3 GHz, of the COBRA II feed horn.

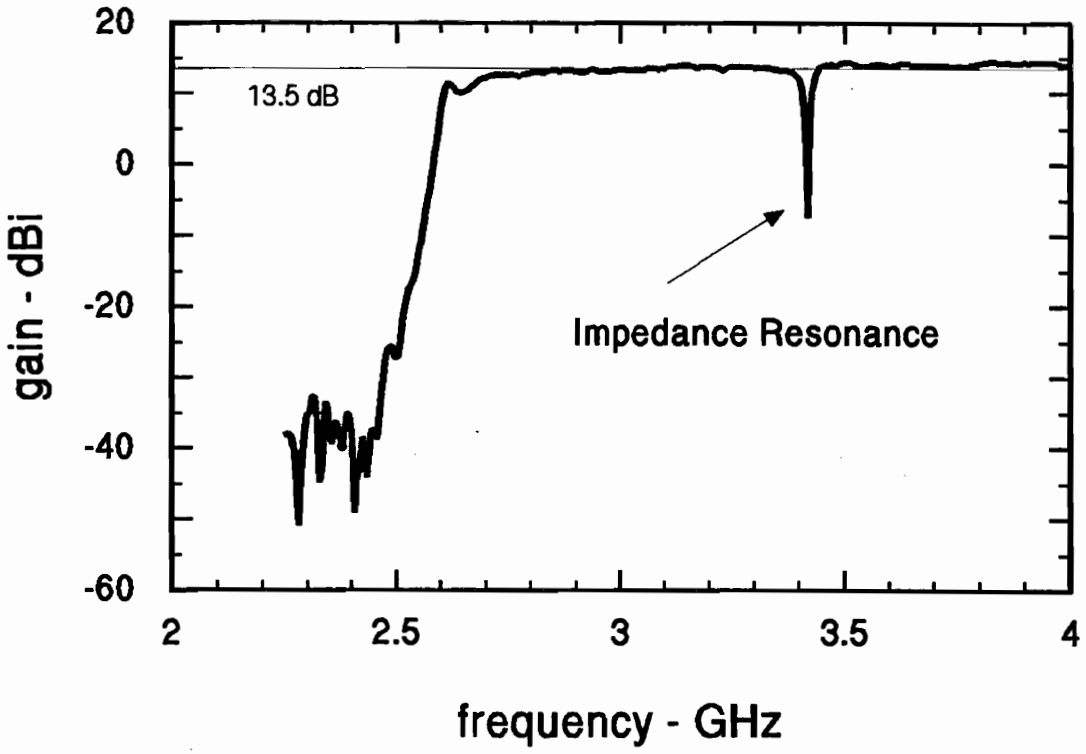

Figure 21. Peak pattern gain of the COBRA II feed horn.

to a nominal value of about 13.5 dBi across the band. Note the narrow resonance region centered about 3.405 GHz where the impedance match to the feed line becomes bad, resulting in a decrease in the apparent measured antenna gain. This artifact can be removed by appropriate design of the feed element.

5.3 N = 1 Patterns

There are four possible (nominal) positions for the COBRA II antenna petals. When all four petals occupy the same position, the antenna is referred to as being in the N = 1 position. When so configured there is no modification of the phase of the incident waveform, and consequently the radiated pattern retains the characteristic null on boresight.

Shown in Figure 22 is the measured azimuthal pattern, taken at a frequency of 3 GHz, of the COBRA II when in the N = 1 configuration. For this case all petals are in the first position (positions 0, 1, 2 and 3 are possible). The peak pattern gain is approximately 26.5 dB, the pattern peak occurs at about $\phi = 3^{\circ}$, and the main lobe half power (–3 dB) beamwidth is approximately 3°. Some asymmetry is observable in the pattern, but for the most part the pattern exhibits the expected properties. In Figure 23 is plotted the azimuthal pattern of the COBRA II about boresight for the four possible petal positions of the N = 1 configuration. Ideally, these curves would overlay each other exactly, but some slight variation is noticeable. This is attributable to

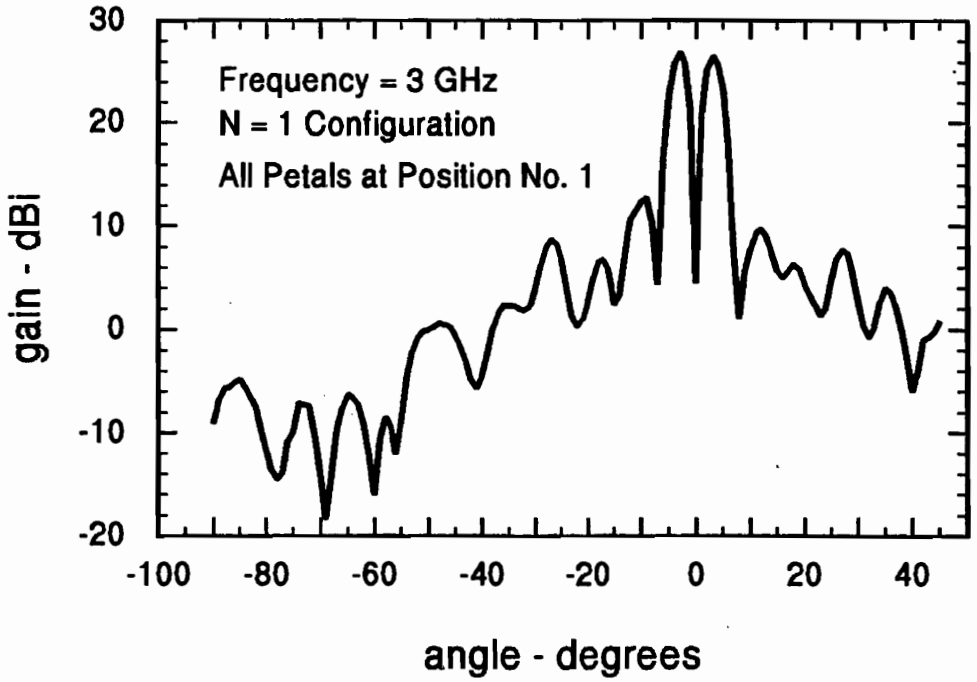

Figure 22. **The azimuthal pattern of the COBRA II configured for N = 1, all petals at position no. 1. The patterns were taken at 3 GHz with a horizontal transmit polarization**

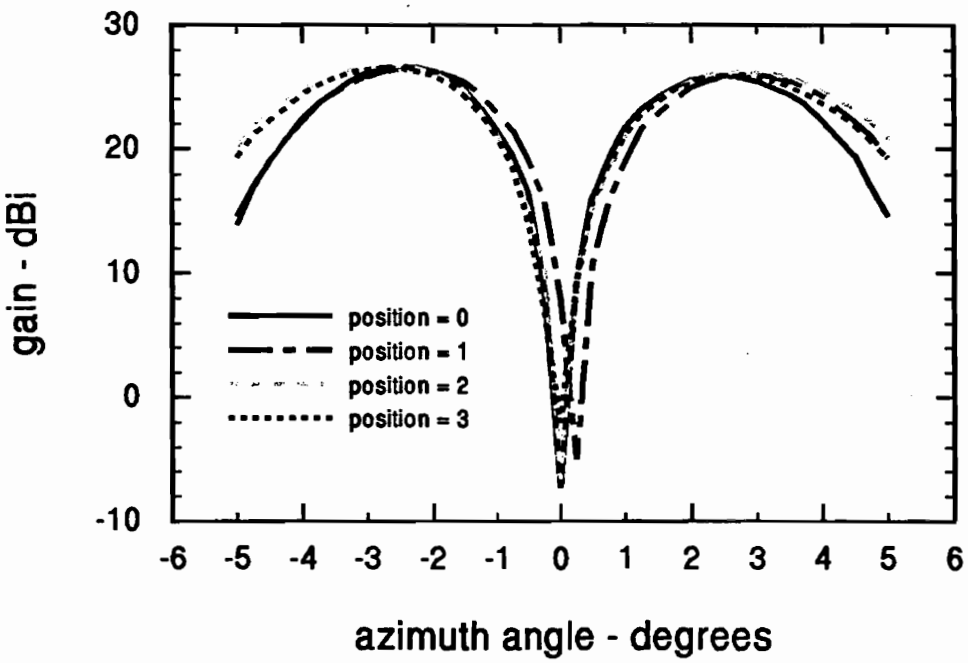

Figure 23. **The azimuthal pattern of the COBRA II configured for N = 1 at all four possible petal positions. The patterns were taken at 3 GHz with a horizontal transmit polarization.**

the defocusing effects caused by the location of the petals at positions other than the first position (nominal), and by alignment errors in the petals. These errors produce effects that are more pronounced in the N = 2 and N = 4 configurations, as the associated data presented later will show. Figure 24 shows the peak pattern gain of the COBRA II N = 1 configuration as a function of frequency. All petals were at Position 1. Except that the gain values are higher (26.5 dB), the characteristic resembles that of the feed horn (Figure 21) as expected.

5.4 N = 2 Patterns

As described earlier, the main reflector of the COBRA was cut into four equivalent sectors or petals. The positioning system is capable of aligning each petal in one of four positions. Assuming that an observer is looking into the segmented main reflector, these ideas of sector and position number are illustrated in Figure 25. For the COBRA II to be in an N = 2 configuration means that there is a single cut / shift in the main reflector contour, and there are twelve possible configurations for the N = 2 COBRA II. Four cases are illustrated in Figure 26. All possible configurations are summarized in Table 1, there the petal positions and resulting boresight polarizations are indicated for the 12 cases.

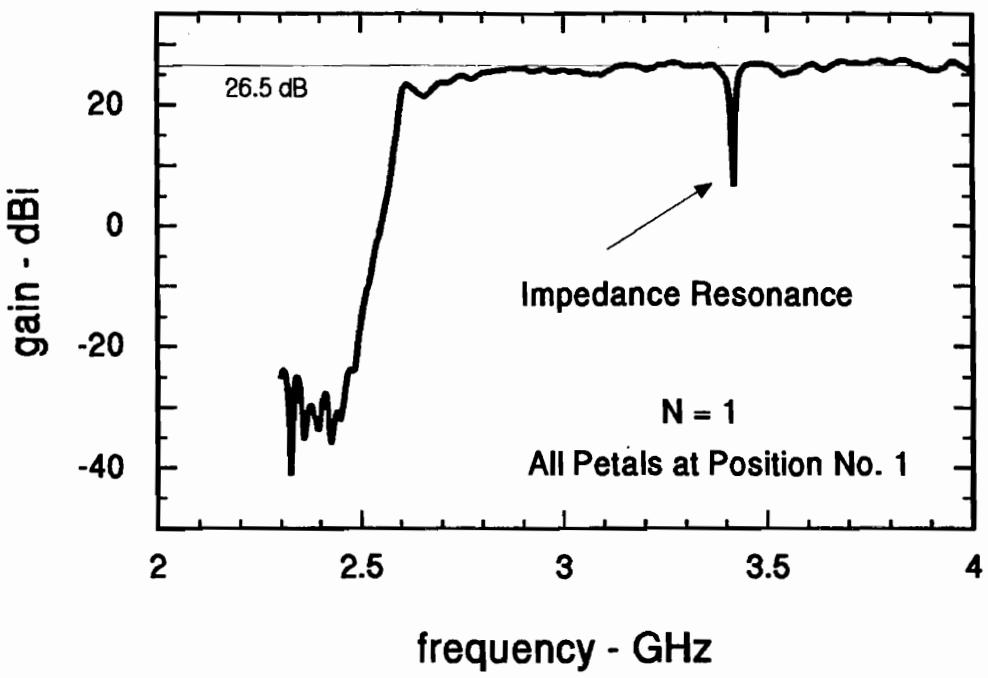

Figure 24. The peak pattern gain as a function of frequency over the 2.3 – 4 GHz frequency band. The COBRA II is configured for N = 1 at all four possible petal positions, and the patterns were taken at 3 GHz with a horizontal transmit polarization

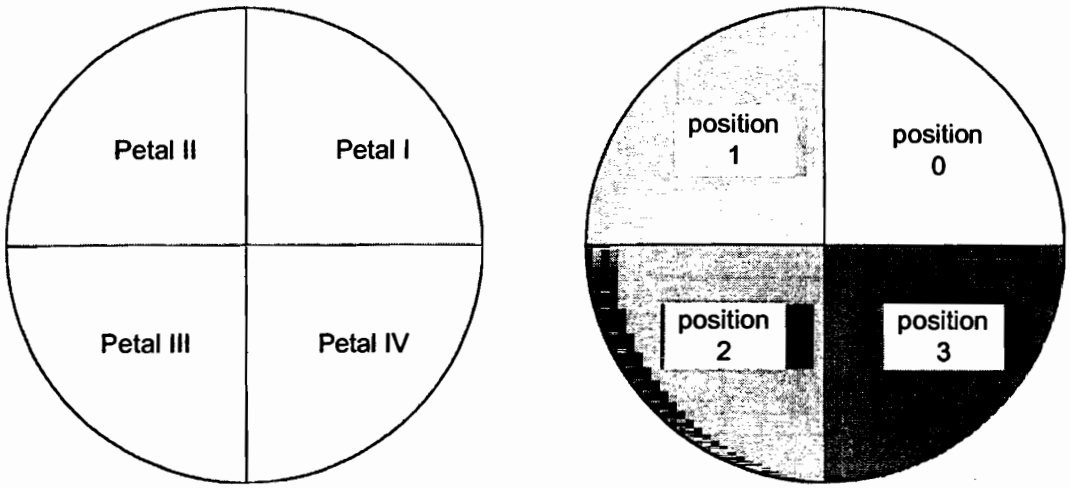

Figure 25. **The profile of the COBRA II main reflector: (a) it is cut into four equivalent sectors or petals; (b) each of the possible four petal positions is represented by a gray scale.**

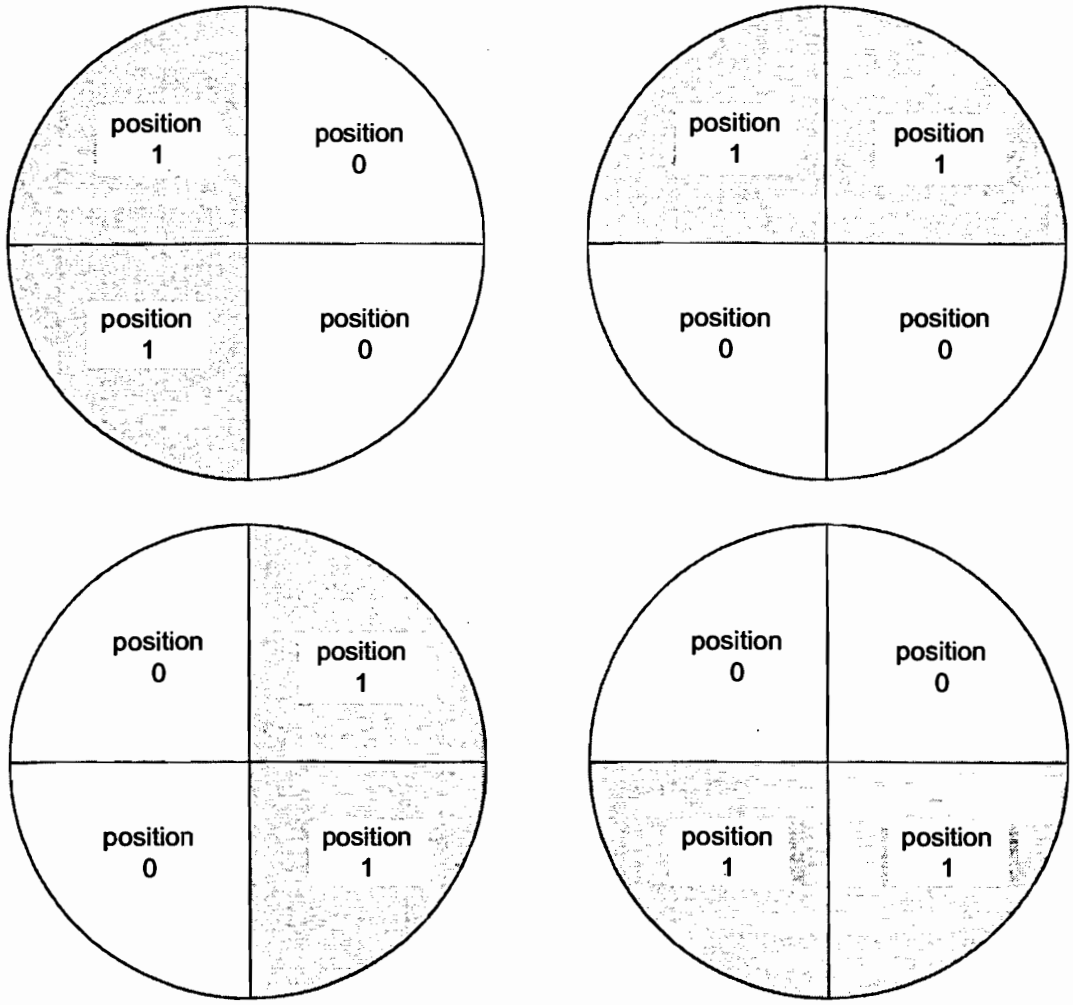

Figure 26. **Four possible petal configurations for an N = 2 COBRA II.**

Table 1. Possible petal positions for the N = 2 configured COBRA II.

Petal I Position	Petal II Position	Petal III Position	Petal IV Position	Boresight Polarization
0	0	1	1	V
1	1	2	2	V
2	2	3	3	V
1	1	0	0	V
2	2	1	1	V
3	3	2	2	V
0	1	1	0	H
1	2	2	1	H
2	3	3	2	H
1	0	0	1	H
2	1	1	2	H
3	2	2	3	H

The above discussion was to illustrate the many different configuration combinations that are possible with the COBRA II. A great deal of data was taken for all possible N = 2 configurations, but just representative data sets will be presented below.

For the N = 2 case, the boresight polarization is linear, and the polarization is either vertical or horizontal depending on the specific positioning of the petals. Below is presented data characteristic of the N = 2 configuration for the vertically and horizontally polarized boresight field.

5.4.1 Horizontally Polarized Boresight Field

To produce a horizontally polarized boresight field, the COBRA II must be configured in one of the ways described in Table 1. For the measurements presented below, the configuration was: Petal I = Position 0, Petal II = Position 1, Petal III = Position 1 and Petal IV = Position 0. The azimuthal pattern of the horizontal component of the radiated field was measured at 3 GHz, and the resulting pattern is shown in Figure 27. The peak gain is seen to be about 28 dB, with side lobe levels of 18.7 and 25.3 dB. Though the pattern has symmetry in other respects, the asymmetry (particularly in the level) was noticed in all measurements.

The peak pattern gain as a function of frequency was measured and is shown in Figure 28. The characteristic exhibits many of the same features found in the feed horn and N = 1 frequency sweeps, but with more structure. This additional structure is mainly due to the separation of the petals, but also to multi-path problems. The azimuthal patterns of the horizontal component of the radiated field at selected frequencies across the band are shown in Figure 29. One notes that pattern characteristics (peak gain) remain fairly constant, except for the extreme ends of the frequency band. A closer look at the boresight pattern at the selected frequencies is shown in Figure 30.

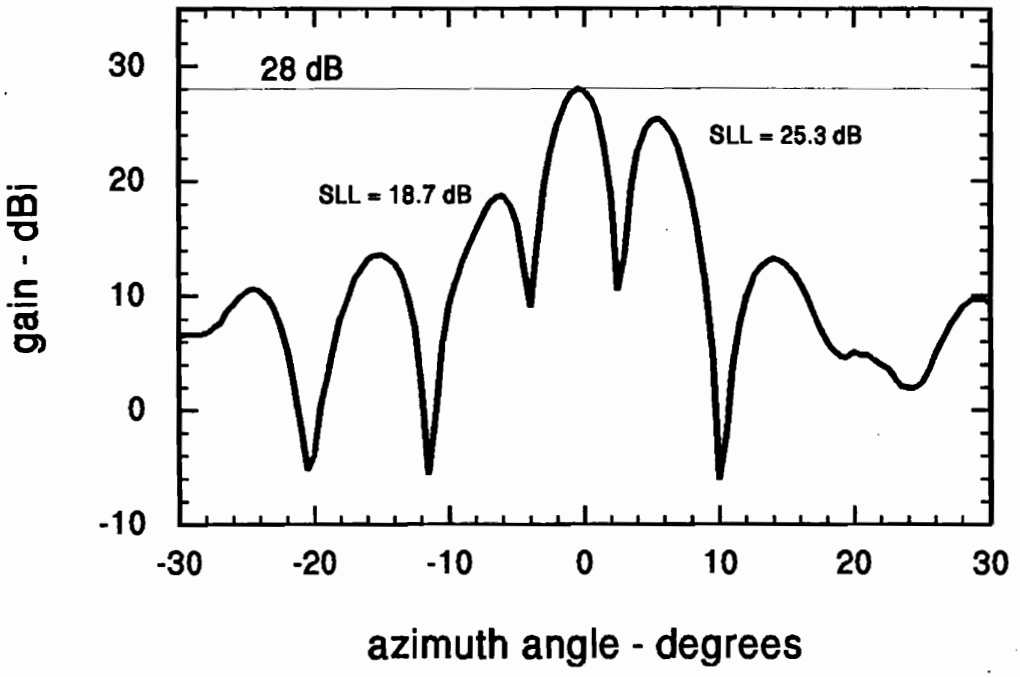

Figure 27. **The azimuthal pattern of the horizontally polarized component of the radiated field of the COBRA II (N = 2).**

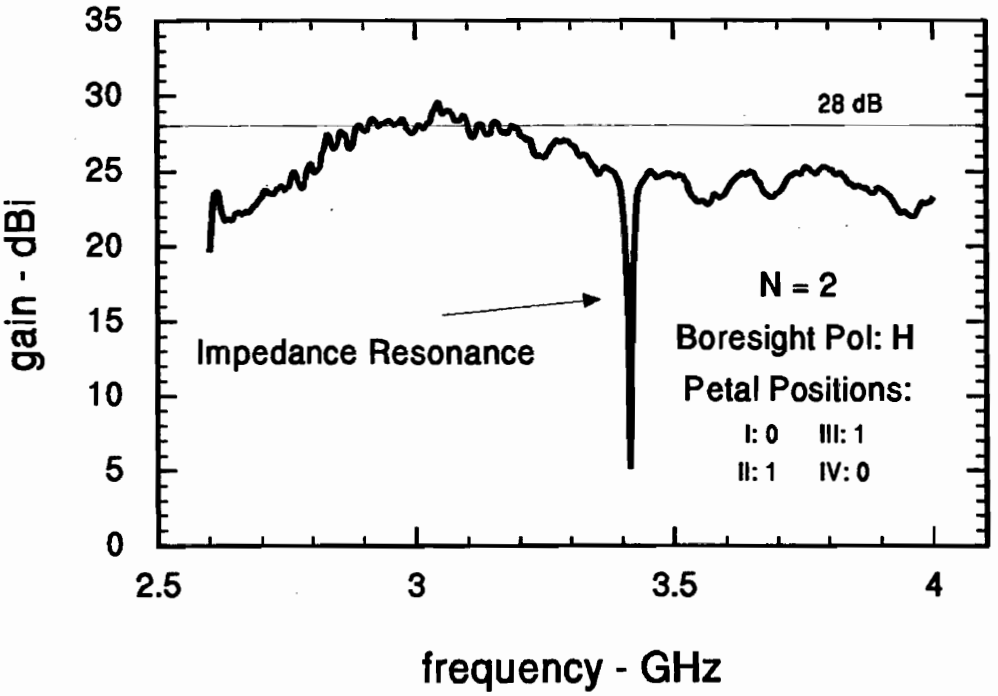

Figure 28. **The pattern peak of the horizontally polarized component of the radiated field of the COBRA II (N = 2) as a function of frequency from 2.6 – 4 GHz.**

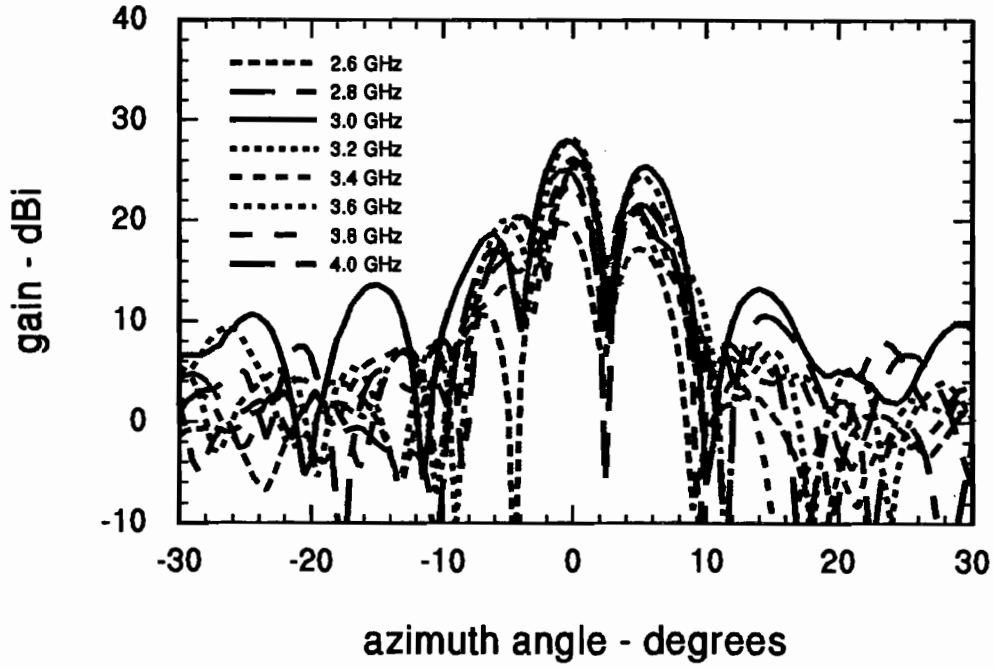

Figure 29. **The azimuthal patterns of the horizontally polarized components of the radiated field of the COBRA II (N = 2) for the frequencies: 2.6, 2.8, 3.0, 3.2, 3.4, 3.6, 3.8, and 4.0 GHz.**

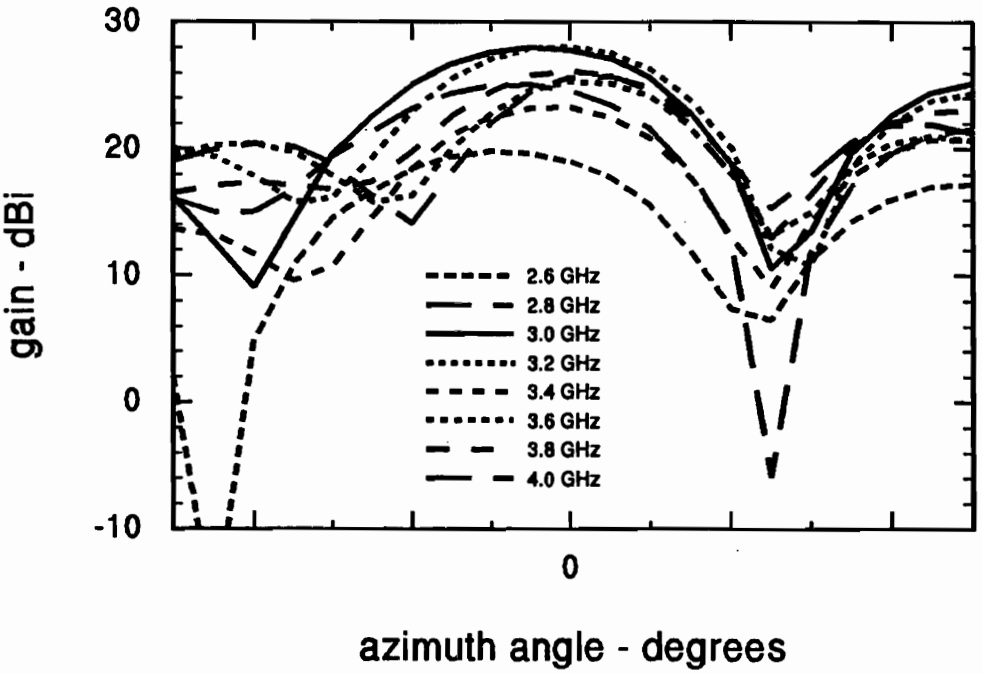

Figure 30. **The azimuthal patterns of the horizontally polarized components of the radiated field of the COBRA II (N = 2) for the frequencies: 2.6, 2.8, 3.0, 3.2, 3.4, 3.6, 3.8, and 4.0 GHz. Close up of boresight field.**

5.4.2 Vertically Polarized Boresight Field

To produce a vertically polarized boresight field, the COBRA II must be configured in one of the ways described in Table 1. For the measurements presented below, the configuration was: Petal I = Position 0, Petal II = Position 0, Petal III = Position 1 and Petal IV = Position 1. The azimuthal pattern of the horizontal component of the radiated field was measured at 3 GHz, and the resulting pattern is shown in Figure 31. The peak gain is seen to be about 27 dB, with side lobe levels of 13.1 and 6.5 dB. As before, the pattern has symmetry in other respects, but the asymmetry in the side lobe levels is apparent. Also of interest are the side lobe levels. They are significantly reduced from the levels of the horizontally polarized case (see Figure 27). This characteristic, much higher side lobe levels in one of the principal planes, was noticed in all N = 2 and N = 4 measurements.

The peak pattern gain as a function of frequency was measured, and is shown in Figure 32. The characteristic exhibits many of the same features found in the horizontally polarized N = 2 frequency sweep. The azimuthal patterns of the vertical component of the radiated field at selected frequencies across the band are shown in Figure 33. One notes that pattern characteristics (peak gain) remain fairly constant, except for the extreme ends of the frequency band. A closer look at the boresight pattern at the selected frequencies is shown in Figure 34.

Finally, it was noticed that the beam direction changed slightly as the COBRA II was cycled though all of the possible configurations. This indicates a slight misalignment of the petals and is partially responsible for reducing the measured gain values. These effects were even more pronounced in the N = 4 measured data.

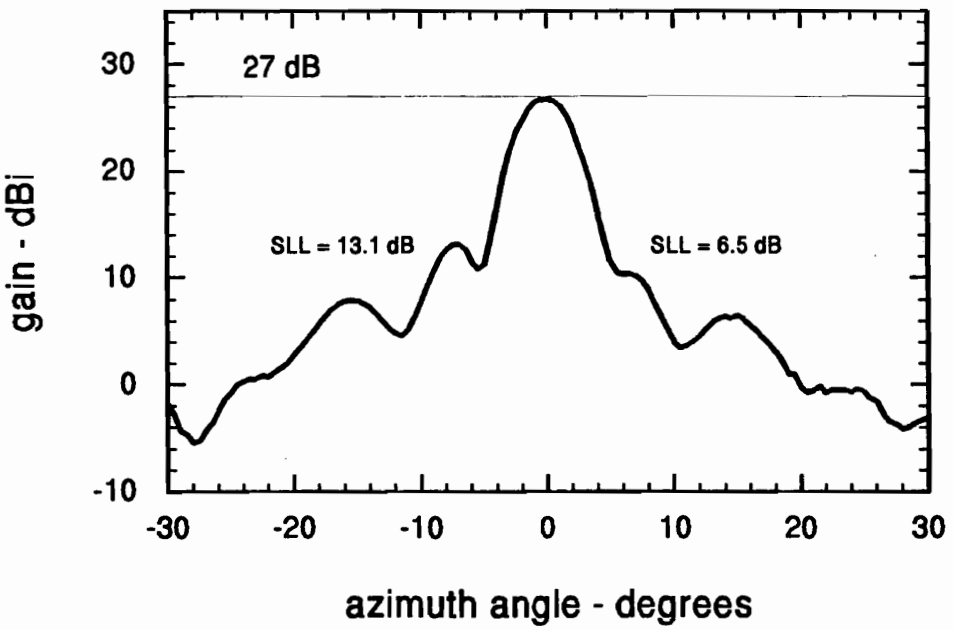

Figure 31. The azimuthal pattern of the vertically polarized component of the radiated field of the COBRA II (N = 2).

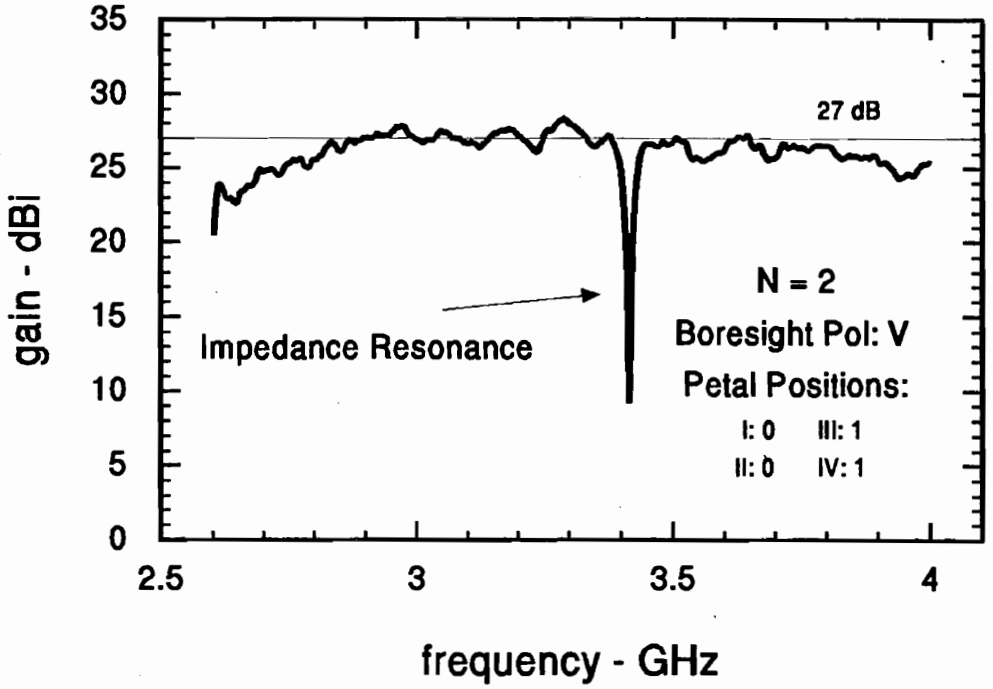

Figure 32. **The pattern peak of the vertically polarized component of the radiated field of the COBRA II (N = 2) as a function of frequency from 2.6 – 4 GHz.**

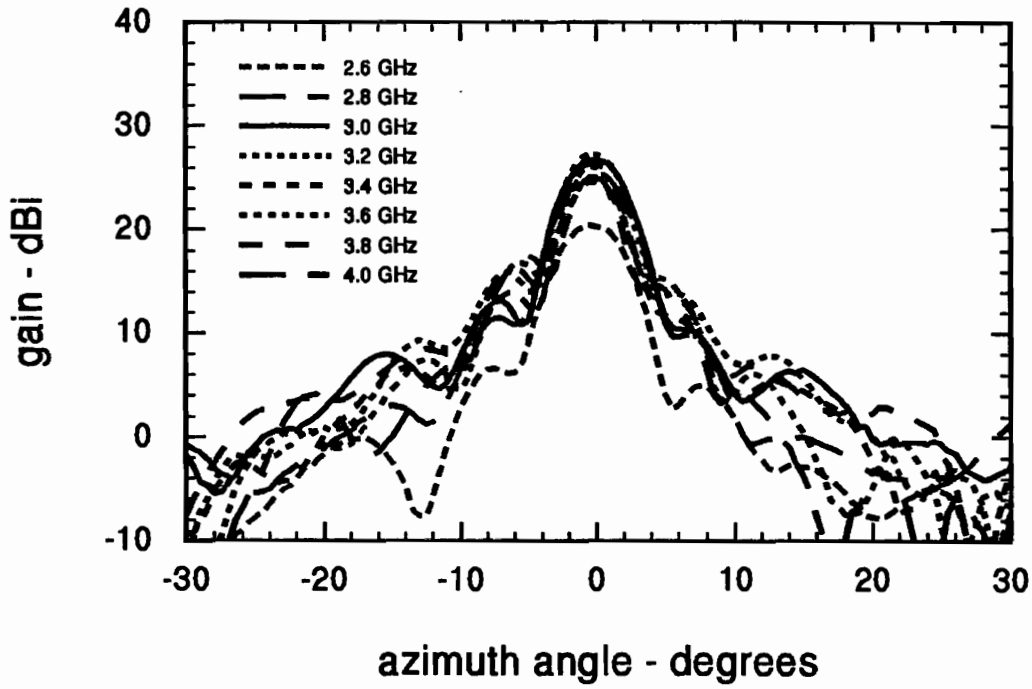

Figure 33. **The azimuthal patterns of the vertically polarized components of the radiated field of the COBRA II (N = 2) for the frequencies: 2.6, 2.8, 3.0, 3.2, 3.4, 3.6, 3.8, and 4.0 GHz.**

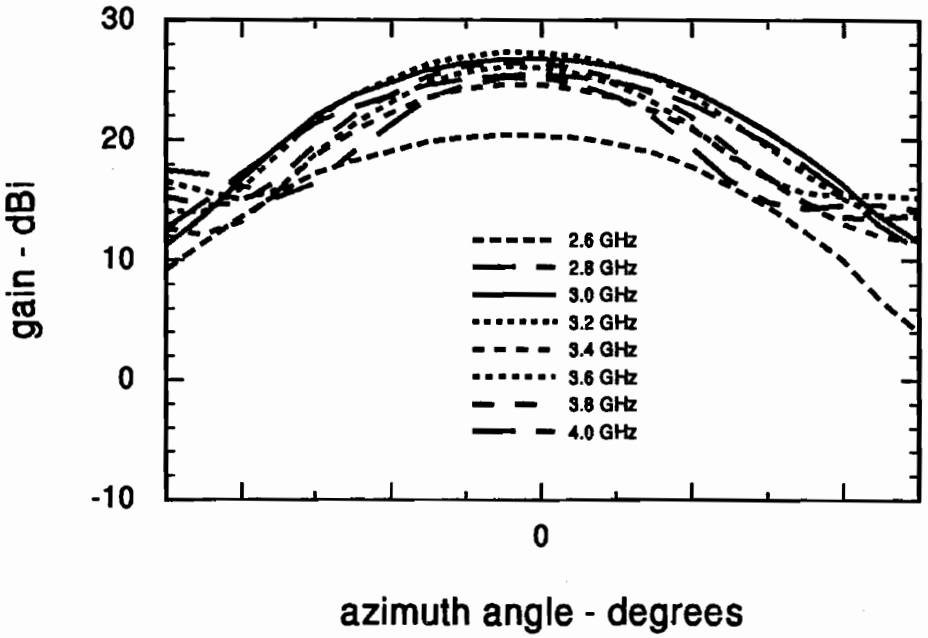

Figure 34. The azimuthal patterns of the vertically polarized components of the radiated field of the COBRA II (N = 2) for the frequencies: 2.6, 2.8, 3.0, 3.2, 3.4, 3.6, 3.8, and 4.0 GHz. Close up of boresight field.

5.5 N = 4 Patterns

For the COBRA II to be in an N = 4 configuration means that the four petals of the main reflector are at different positions, with each petal being a single position forward or behind the adjacent petal. Consequently, there are eight possible configurations for the N = 4 COBRA II. Two cases are illustrated in Figure 35. For the case where the petals move forward one position in a counterclockwise fashion, the resulting boresight polarization will be left-hand circular polarization (LHCP). For the case where the petals move forward one position in a clockwise fashion, the resulting boresight polarization will be right-hand circular polarization (RHCP). All possible configurations are summarized in Table 2. There, the petal positions and resulting boresight polarizations are indicated for the eight cases. As was the case for the N = 2 measurements, a great deal of data was taken for all possible N = 4 configurations, but just representative data sets will be presented below. Also, the boresight field is circularly polarized for the N = 4 case, but the measurements were made with linearly polarized probes. Consequently, the data presented below are associated with a single polarization of the COBRA II (N = 4) field (horizontal or vertical). The next section presents measurements that verify the circularly polarized nature of the boresight field. Before the data is presented, a brief explanation of the measurement system is presented in the next paragraph.

The Air Force Research Laboratory / Directed Energy narrowband antenna range measurement system [Ref. 11 and 12] was used to measure the radiation characteristics of the COBRA II antenna. The system utilizes a Hewlett-Packard 8510 network analyzer and a custom s-parameter test set, and uses a comparison measurement technique to measure the pattern and

gain of an antenna under test (AUT). Typically, the AUT and a system calibration (CAL) antenna are configured as receive antennas, and a third antenna is operated in the transmit (TX) mode. The CAL and TX antennas for this test were two standard gain horn antennas (Narda 644) which are linearly polarized antennas. Consequently, even though the N = 4 configured COBRA II exhibits circular polarization properties, just the response of the COBRA II to a single linear polarization was measured at a time. In the data presented below, just the response of the COBRA II to a linearly polarized incident field is presented. After measurements of the response of the COBRA II to two orthogonal polarizations were made, certain inferences (total system gain) as to the transmitting properties were made.

Figure 36 shows the azimuthal pattern of the N = 4 – configured COBRA II. The petal positions were: Petal I = Position 2, Petal II = Position 3, Petal III = Position 0 and Petal IV = Position 1. The pattern was measured at 3 GHz with a vertically polarized transmit antenna. The peak gain is seen to be about 24 dB, with no distinguishable side lobes. Assuming the other polarization carries an equivalent amount of power, the total system gain would be approximately 27 dB. As mentioned previously, multi-path problems did affect the measurements. Figure 37 shows the pattern peak gain of the N = 4 configured COBRA II for the transmit antenna oriented for vertical and horizontal polarization. It can be shown that the horizontal and vertical reflection coefficients for lossy dielectric surfaces (cement, soil, etc.) at other than grazing angles of incidence are of opposite sign. Then this figure indicates a bound on the possible error in the measurement. Also, since the two measurements agree at 3 GHz, it seems to indicate that the error at that frequency is minimal.

Measurements of the azimuthal pattern of the N = 4 – configured COBRA II were made with the transmit horn both horizontally and vertically polarized. These patterns are shown together in Figure 38. One notes that the side lobe levels are high and the main beam is narrow for one polarization, while the side lobe levels are low and the main beam is wide for the other polarization.

The azimuthal receive patterns of the of the N = 4 – configured COBRA II, for a vertically polarized incident field, at selected frequencies across the band are shown in Figure 39. One notes that pattern characteristics (peak gain) remain fairly constant, except for the extreme ends of the frequency band. A closer look at the boresight pattern at the selected frequencies is shown in Figure 40. The azimuthal receive patterns of the of the N = 4 – configured COBRA II, for a horizontally polarized incident field, at selected frequencies across the band are shown in Figure 41. Contrary to the previous case, one notes that pattern characteristics (peak gain) are extremely sensitive to frequency. A closer look at the boresight pattern at the selected frequencies is shown in Figure 42. All of this data was taken at a single petal position and configuration. In other words, the petal positions were not adjusted as the frequency was changed.

As was the case for the N = 2 configuration, it was noticed that the beam direction changed slightly as the COBRA II was cycled though all of the possible configurations. This indicates a slight misalignment of the petals and is partially responsible for reducing the measured gain values. These effects were more pronounced for the N = 4 measured data.

Table 2. Possible petal positions for the N = 4 configured COBRA II.

Petal I Position	Petal II Position	Petal III Position	Petal IV Position	Boresight Polarization
0	1	2	3	LHCP
1	2	3	0	LHCP
2	3	0	1	LHCP
3	0	1	2	LHCP
0	3	2	1	RHCP
1	0	3	2	RHCP
2	1	0	3	RHCP
3	2	1	0	RHCP

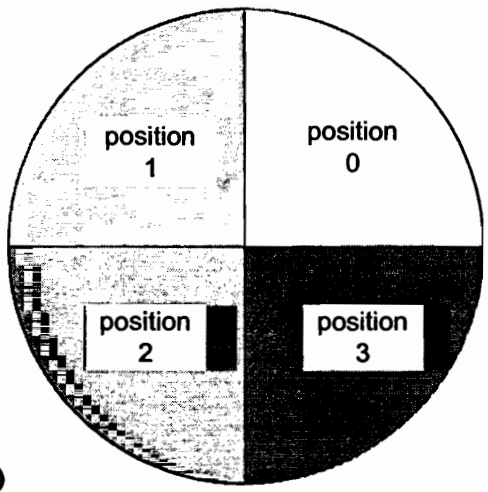

(a)

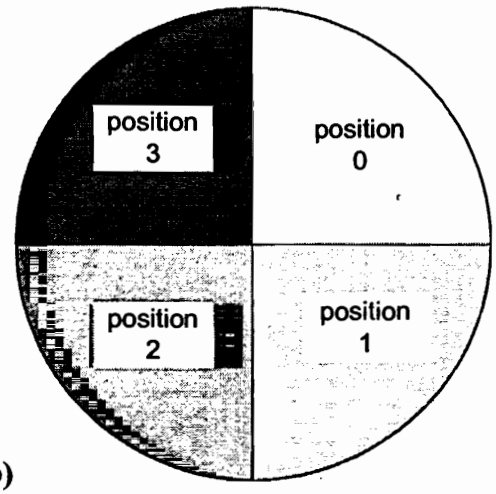

(b)

Figure 35. Two possible petal configurations for a N = 4 COBRA II: (a) produces LHCP; and (b) produces RHCP. The perspective is looking into the main reflector of the COBRA II.

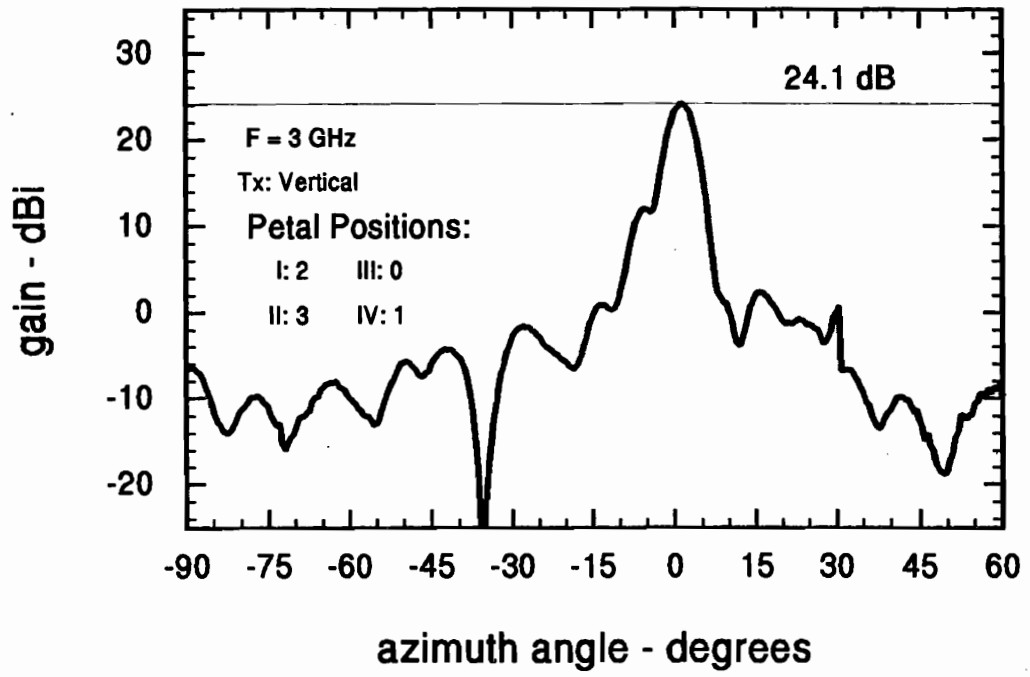

Figure 36. **The azimuthal pattern of the N = 4 - configured COBRA II (operated in receive mode). The transmit antenna was oriented for vertical polarization.**

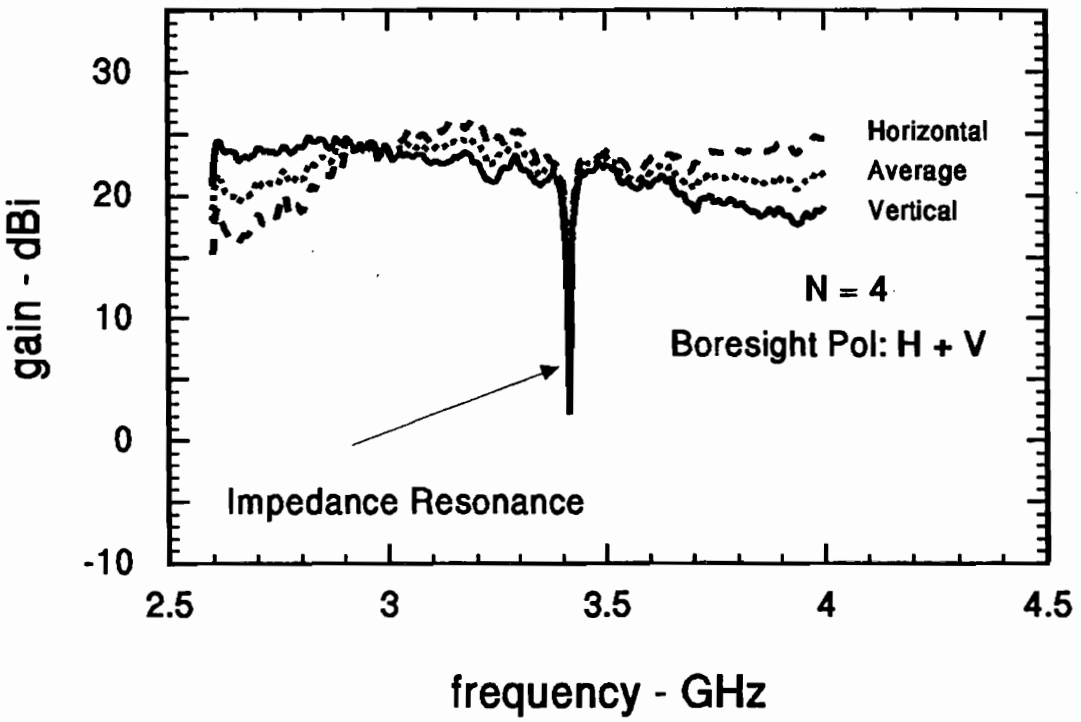

Figure 37. **The pattern peak gain of the N = 4 configured COBRA II (operated in receive mode). The transmit antenna was oriented for vertical polarization, and then prior to the second measurement for horizontal polarization.**

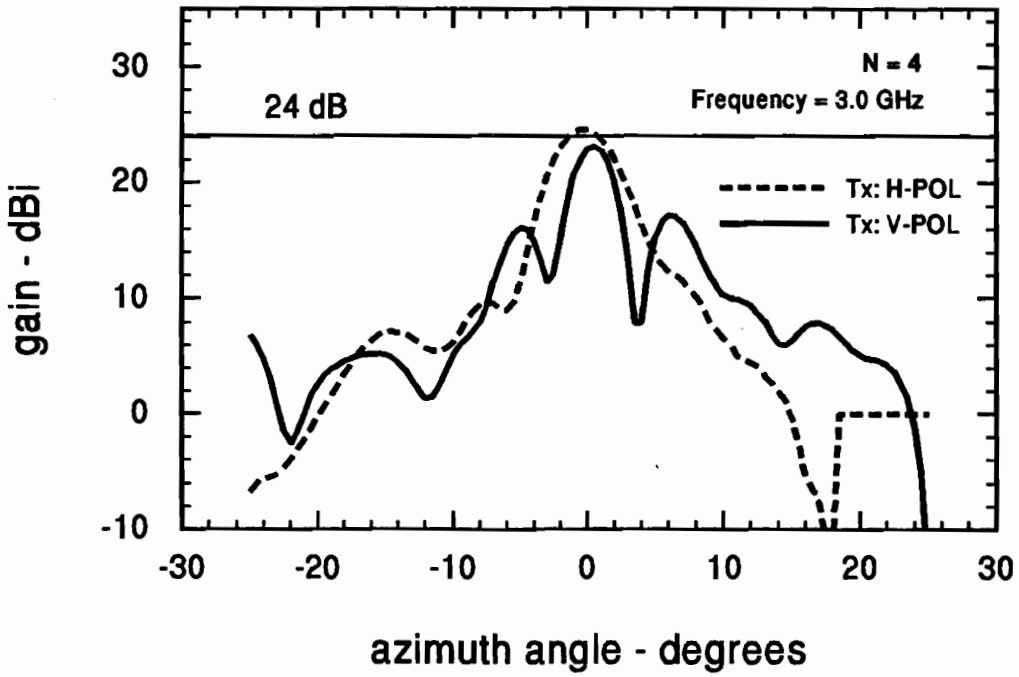

Figure 38. **The azimuthal receiver pattern of the N = 4 configured COBRA II for the transmit antenna oriented for vertical, and then horizontal polarization.**

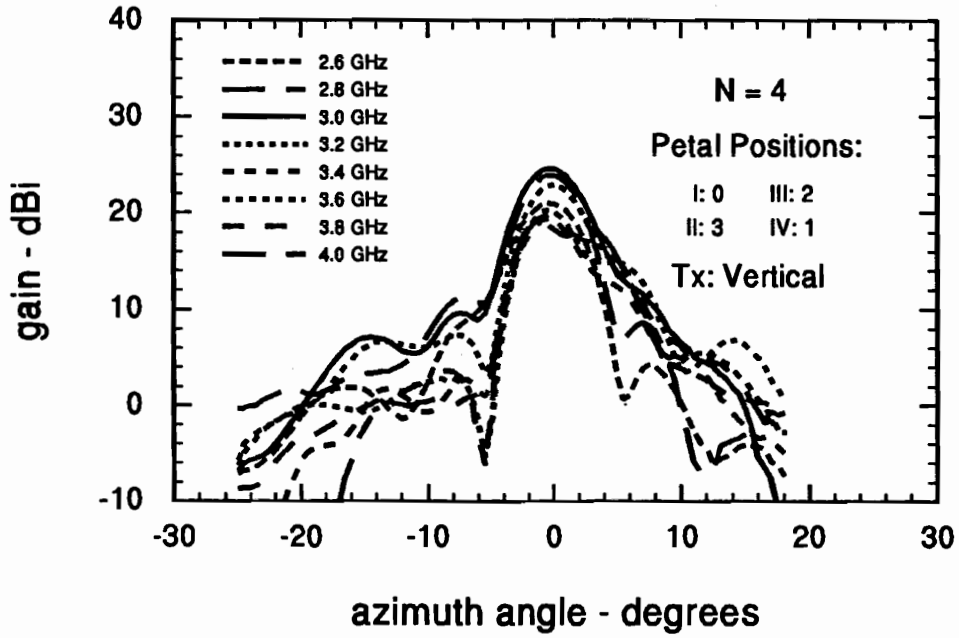

Figure 39. **The azimuthal patterns of the radiated field of the COBRA II (N = 4) for the frequencies: 2.6, 2.8, 3.0, 3.2, 3.4, 3.6, 3.8, and 4.0 GHz. The transmit antenna was oriented to produce a vertically polarized field.**

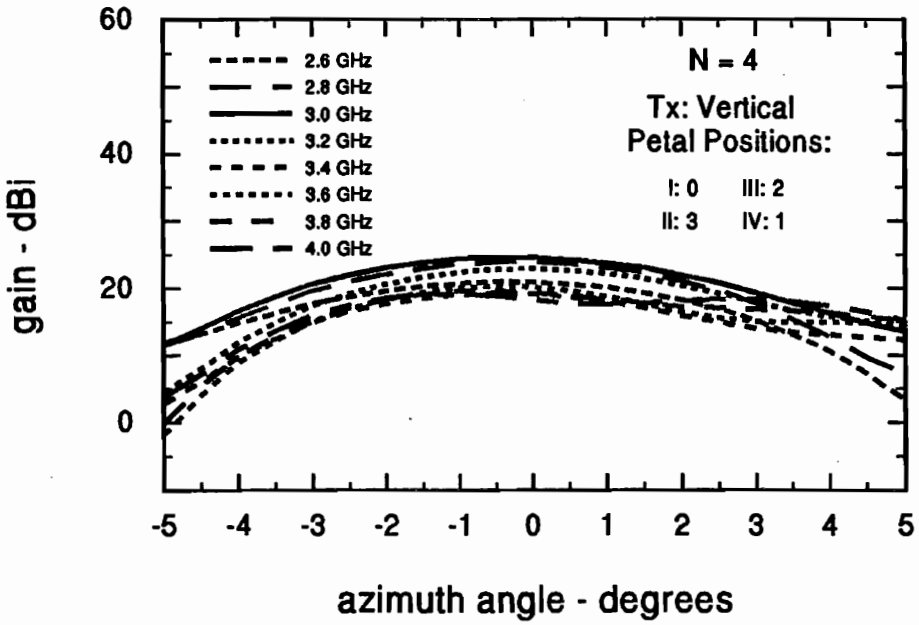

Figure 40. **The azimuthal patterns of the radiated field of the COBRA II (N = 4) for the frequencies: 2.6, 2.8, 3.0, 3.2, 3.4, 3.6, 3.8, and 4.0 GHz. Close up of boresight field. The transmit antenna was oriented to produce a vertically polarized field.**

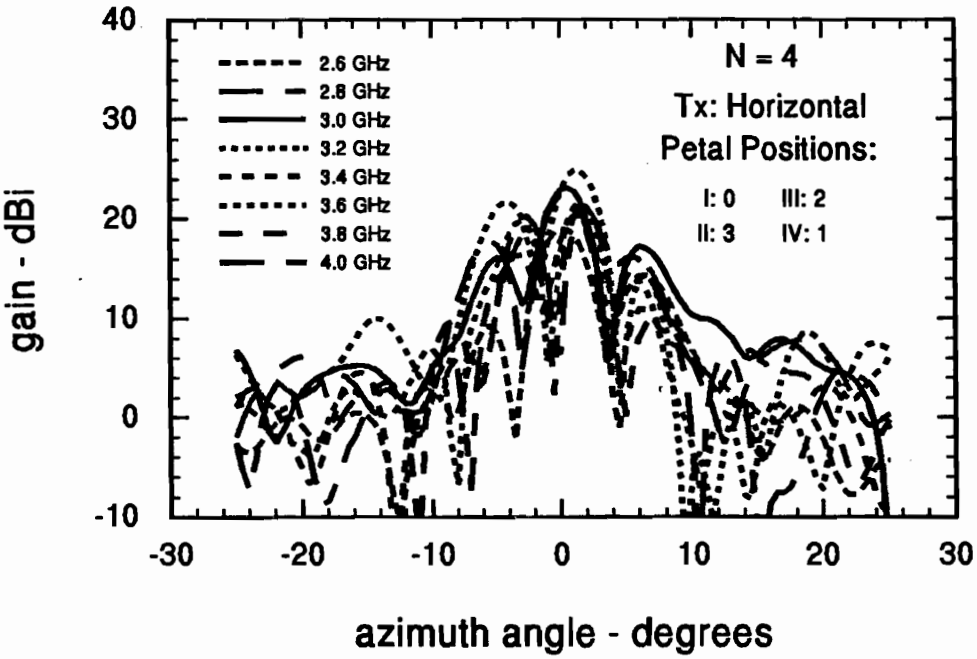

Figure 41. **The azimuthal receive patterns of the radiated field of the COBRA II (N = 4) for the frequencies: 2.6, 2.8, 3.0, 3.2, 3.4, 3.6, 3.8, and 4.0 GHz. The transmit antenna was oriented to produce a horizontally polarized field.**

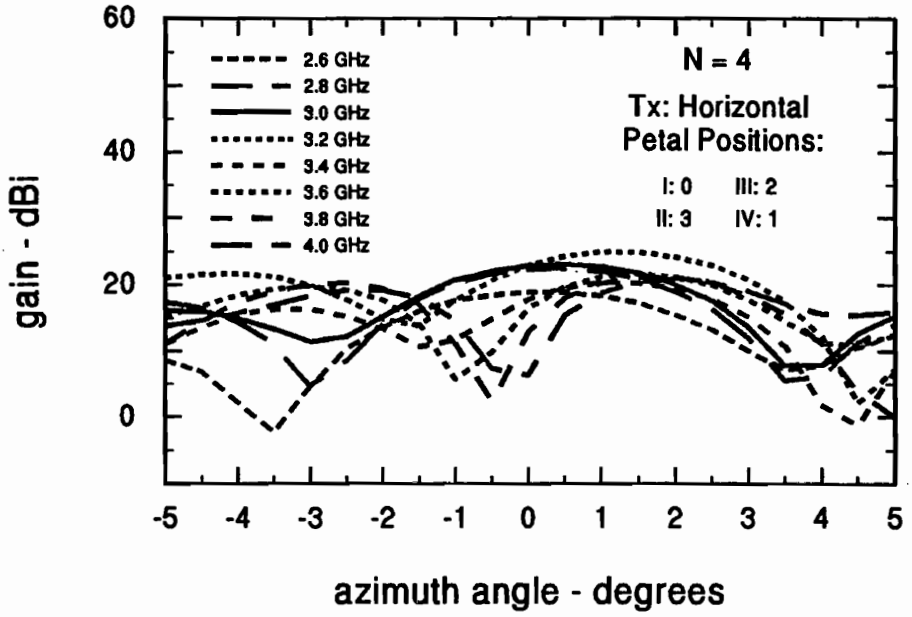

Figure 42. The azimuthal patterns of the radiated field of the COBRA II (N = 4) for the frequencies: 2.6, 2.8, 3.0, 3.2, 3.4, 3.6, 3.8, and 4.0 GHz. Close up of boresight field. The transmit antenna was oriented to produce a horizontally polarized field.

5.6 N = 4 Boresight Phase Relationships

To verify that the COBRA II (N = 4 configuration) radiated boresight field is circularly polarized, the magnitude of the vertical and horizontal polarizations must be equal and the phase difference between the two must be 90 degrees. The magnitude and phase of the boresight field were measured directly in the manner described in [Ref. 13]. The ratio (dB) of the horizontal and vertical components of the boresight field is shown in Figure 43. A value of 0 dB indicates equal magnitudes of the components, and this is observed at the design center frequency of 3 GHz. It is also seen that the relative magnitudes of the two orthogonal polarizations stay with ± 3 dB across practically the entire measurement band.

The difference of the phase (degrees) of the horizontal and vertical components of the boresight field is shown in Figure 44. A value of 90 degrees is required to indicate circular polarization, and this is observed at the design center frequency of 3 GHz. It is also seen that the phase difference stays with ± 10 degrees across practically the entire measurement band. Again, all of this data was taken at a single petal configuration, the petal positions were not adjusted as the frequency was changed. These measured properties indicate that the bandwidth of the COBRA II (N = 4 configuration) is approximately 2.4 GHz – 3.7 GHz, or almost 45%,

$$BW = \frac{f_{High} - f_{Low}}{f_{Center}} = \frac{3.7 - 2.4}{3} \times 100\% = 43.33\%,$$

which is somewhat surprising considering the nature of the tuned surfaces of the antenna.

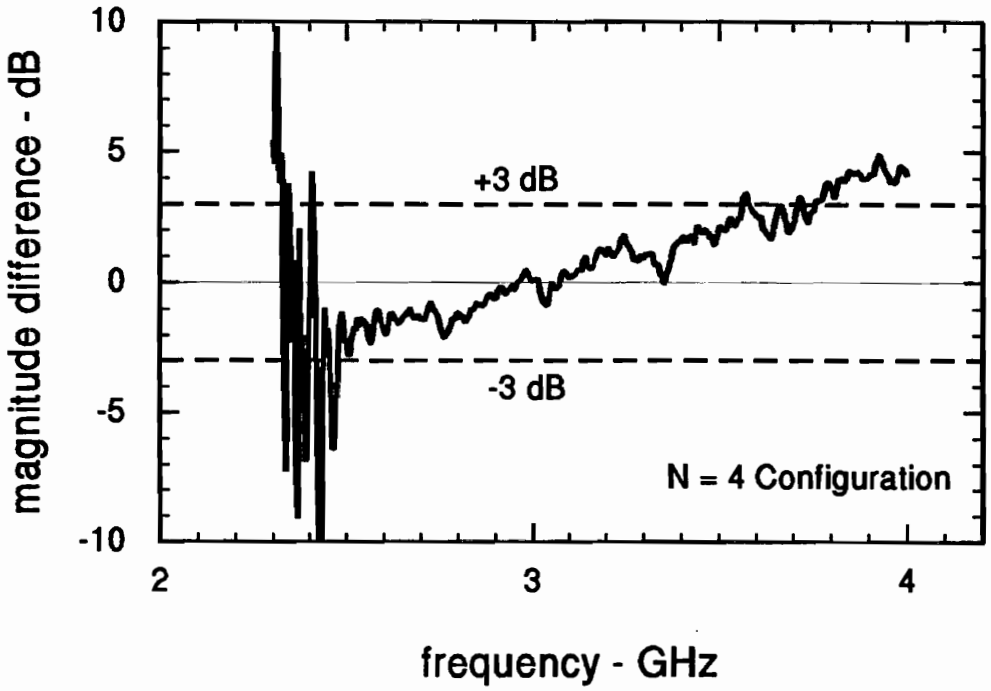

Figure 43. **The measured ratio of the magnitudes of the vertical and horizontal components of the radiated boresight field of the COBRA II (N = 4).**

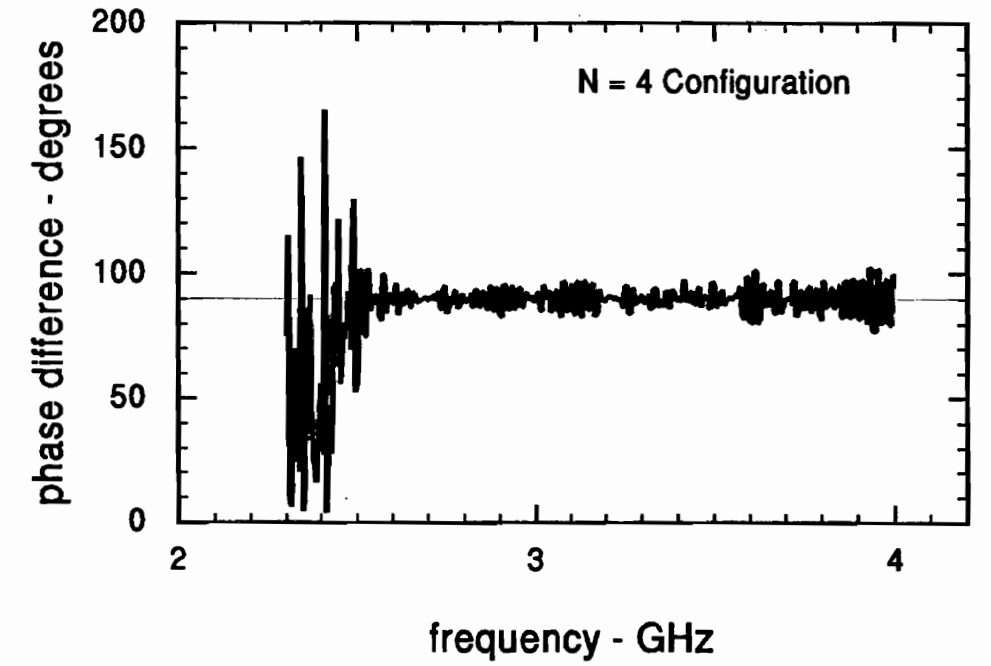

Figure 44. **The measured difference of the phase of the vertical and horizontal components of the radiated boresight field of the COBRA II (N = 4 configuration).**

6. COBRA System Summary and Conclusions

This section gives a summary of the design and measured performance of the COBRA II prototype antenna. A summary of the physical characteristics of the COBRA II prototype is given in Table 3.

The aperture gain is simply $G_{aperture} = 4\pi \frac{Area}{\lambda^2}$. The area of the COBRA II aperture is

$$Area = \pi\left(r_2^{\,2} - r_1^{\,2}\right) - Area_{cut\,out} = \pi\left(r_2^{\,2} - r_1^{\,2}\right) - \left[(62.5 \times 1 \times 2)\left(\frac{2.54\,cm}{in}\right)^2\left(\frac{1\,m}{100\,cm}\right)^2\right] = 1.6752 \text{ m}^2$$

The aperture gain is then

$$G_{aperture} = 4\pi \frac{Area}{\lambda^2} = \frac{4\pi}{(0.1)^2}(1.6752) = 2{,}105\,.$$

Table 3. Summary of the physical characteristics of the COBRA II prototype.

Parameter	Value
Design center frequency	3 GHz
Feed horn mode	TM_{01} circular waveguide mode
Main reflector diameter – usable (actual)	625 inches (68 inches)
Main reflector focal length	16.875 inches
No. of main reflector segments (petals)	4, equally sized
Petal positioning	Asymmetric scissors jack / each petal
Focal length / diameter (main parabolic reflector)	0.26
Subreflector diameter	21 inches
Subreflector eccentricity	1.623
Feed horn aperture diameter	14 inches
Feed horn circular wave guide feed internal diameter	3.5 inches
Reference petal position (petal #1)	Defined as 0.00 inches
Petal # 2 position (ahead of reference)	0.492 inches
Petal # 3 position (ahead of reference)	0.984 inches
Petal # 4 position (ahead of reference)	1.476 inches
Effective focal length of COBRA II	71 inches

The boresight aperture efficiency is then defined as the measured boresight gain divided by the aperture gain η = aperture efficiency $= G_{measured} / G_{aperture} \times 100\%$. The band width is defined as

$$BW = \frac{f_{high} - f_{low}}{f_{center}}$$

A summary of the measured electrical characteristics of the COBRA II prototype in Table 4.

There are a few concluding remarks that can be made about the design and measurement of the COBRA II antenna. First, the COBRA II has demonstrated an end-fire design that is compatible with several high power microwave sources. The antenna was able to transform an azimuthally symmetric aperture mode into one that produces a boresight peak with circular polarization. Second, though the design and manufacture of the COBRA II was conducted carefully, petal positioning was less than perfect. This was noticeable in the manner in which the beam peak moved as a function of the individual petal positioning. This is also the reason that the measured aperture efficiency (low 20%) was somewhat less than anticipated (30%). Finally, the automated petal positioning system demonstrated the ability to rapidly and accurate reposition the petals and adjust the boresight polarization.

Table 4. Summary of the measured electrical characteristics of the COBRA II prototype.

	N = 1	N = 2 (V)	N = 2 (H)	N = 4 (PP1)	N = 4 (PP2)
Peak Gain	26.5 dB	27 dB	28 dB	24 dB (27 dB)	23.5 (26.5 dB)
Beamwidth	3°	8°	4°	8°	4°
Peak SLL	×	13.1 dB	25.3 dB	12 dB	15 dB
Bandwidth		47 %	47 %	30 %	30 %
η = Aperture Eff.	×	23.8 %	29.97 %	11.9 % (23.9 %)	10.63 % (21.22 %)
	N = 4 Boresight polarization magnitude ratio = 1				
	N = 4 Boresight polarization phase difference = 90°				
	Feed horn pattern peak = 13.5 dB				

7. References

1. "Increasing the RF energy per Pulse of an RKO," K. Hendricks, et al, IEEE Trans. on Plasma Science, vol. 26, no. 3, June 1998.
2. "Performance and pulse shortening effects in a 200-kV PASOTRON HPM source," D. Goebel, R. Schumacher and R. Eisenhart, IEEE Trans. on Plasma Science, vol. 26, no. 3, June 1998.
3. "Quasioptical transformer which transforms the waves in a waveguide having circular cross-section into a highly directional wave beam," S. Vlasov and I. Orlava, Radiophys. Quantum Electron,. Vol. 17, 1975.
4. "Analysis of electromagnetic radiation from shaped-end radiators using the Finite Difference Time Domain Method, H. Beggs, et al, IEEE Trans. Antennas and Prop., vol. 41, no. 9, 1993.
5. "Investigation of RF Breakdowns on the MILO," D. Schiffler, et al, IEEE Trans. on Plasma Science, vol. 26, no. 3, June 1998.
6. "Considerations for a GW-level COBRA Antenna Design," C. Courtney, et al, Eighth National Conference on High Power Microwave Technologies, Johns Hopkins University, April 8 – 10, 1997.
7. "Coaxial Beam-Rotating Antenna (COBRA) Concepts," C. Courtney and C. Baum, Sensor and Simulation Note No. 395, April 1996.
8. "Coaxial Beam Rotating Antenna (COBRA) Concepts to Produce Circularly Polarized Field with a Boresight Peak," C. Courtney and C. Baum, Proceedings of the AMEREM 1996 Symposium, Albuquerque, NM.
9. "Concepts and Performance Estimates of the Coaxial Beam Rotating Antenna (COBRA)," C. Courtney, C. Baum, and R. Torres, Proceedings of the IEEE 1996 Symposium on Antennas and Propagation, Baltimore, MD.
10. Thomas Milligan, *Modern Antenna Design*, McGraw-Hill, New York, 1985.
11. "Narrow Band Continuous Wave RF Diagnostic and Data Reduction System – Software User's Manual," VS-610, Voss Scientific, December 1996.
12. "Enhanced Antenna Range System," VS-313, Voss Scientific, January 1994.
13. "Coaxial Beam-Rotating Antenna (COBRA) Prototype Measurements," C. Courtney, et al, Sensor and Simulation Note No. 408, July 1997.